THERMODYNAMICS OF MODEL UNIVERSES

BY

GERALD ALAN REEVES

FACULTY OF MATHEMATICAL STUDIES

UNIVERSITY OF SOUTHAMPTON

Thesis submitted for the degree of Doctor of Philosophy

1983

CONTENTS

UNIVERSITY OF SOUTHAMPTON

ABSTRACT

FACULTY OF MATHEMATICAL STUDIES

MATHEMATICS

Doctor of Philosophy

THERMODYNAMICS OF MODEL UNIVERSES

by Gerald Alan Reeves

The objectives of this research are (1) to examine the general thermodynamics of oscillating and ever expanding universes, and (2) to discuss a relativistic, quantum-mechanical approach for the momentum transfer during electron-photon scattering in the early universe. First, model universes are studied by means of continuum matter-radiation cosmological models and their generalisations (see points (d)-(f) below) as follows : (a) The connection between the matter-radiation interaction and the irreversibility of oscillating models is discussed, and the consequences of various interactions and how they affect the temperature and entropy changes in the model are traced. (b)'Heat death' characteristics (ever expanding case) are also considered. (c) It is shown for the first time that the relativistic equations allow the energy of an oscillating universe to decrease by the end of a cycle. (d) A new model, a continuum-particle model, has been introduced. This model incorporates the continuum interactions and, in addition, includes particle interactions such as annihilation and element formation. (e) It is found, as in earlier models, that energy is gained during the cycle. This corresponds to an entropy generation per baryon of $6{\cdot}4 \times 10^{6}$ k. (f) At the epoch with $T_r = 2{\cdot}70$ K, the model predicts a nonstandard feature, namely a neutrino temperature slightly above this value at $T_{\nu_e} = T_{\nu_\mu} = 2{\cdot}74$ K. All models are illustrated with numerical computations.

Secondly, a comparison is made between the classical Thomson interaction and a relativistic, quantum-mechanical approach, using the Klein-Nishina formula, for the electron-photon scattering interaction. In each case the rate of momentum transfer to the electrons by the radiation is computed numerically for, (i) a single electron moving through blackbody radiation; and (ii) an equilibrium distribution of electrons interacting with blackboby radiation. The dependence of the transfer rates on temperature and electron velocity was also studied. The Thomson scattering transfer rate was in good agreement with the Klein-Nishina transfer rate at temperatures $T < 10^{7}$ K, but at higher temperatures the Klein-Nishina momentum exchange departed from the corresponding classical Thomson prediction. Many cosmological models begin at high temperatures so the Klein-Nishina interaction ought to be used in such studies.

ACKNOWLEDGEMENTS

I would like to thank Professor Peter Landsberg for encouragement and many helpful discussions during the course of this research, and to Christopher Nash for carefully drawing the diagrams. Financial support from the Science and Engineering Research Council is gratefully acknowledged.

CHAPTER ONE

GENERAL INTRODUCTION

GENERAL INTRODUCTION

1.1 Historical and observational background; the standard model

Astronomy and cosmology are often given the distinction of being the oldest sciences. From earliest times man has been curious about the universe he finds himself in and it was the Greeks, around the second century B.C., who first investigated the idea of an infinite universe. The Greeks made systematic measurements of the heavens and were able to predict the position of the celestial objects. They proposed that the Sun, Moon, and planets were attached to spheres which rotated at different rates with respect to each other, and which in turn rotated about the Earth.

The principle of a geocentric world system was retained until the sixteenth century when Copernicus argued for a heliocentric world system. The Copernican view was quickly given a quantitative basis following the discovery of Kepler's laws of planetary motion and Newton's law of gravitation.

The next major advance in cosmology began with the advent in 1916 of Einstein's general theory of relativity. By combining inertial and gravitational forces within its framework, general relativity provided a relativistic theory of gravitation, and this soon led to a relativistic interpretation of cosmology.

The aim of relativistic cosmology was to describe the dynamical structure of the universe as a whole by taking gravitation, as interpreted by general relativity, as the dominant interaction. To try and solve the problem in its complete generality by incorporating all the planets, stars, galaxies, etc. into the model, was clearly impractical and probably insoluble. To simplify the task local irregularities and details were smoothed out, and attention

could then be concentrated on simply the gross features of the universe.

In 1922 A.Friedmann discovered a solution of the general relativity equations by imposing the hypothesis that the material content of the universe was homogeneous and isotropic in distribution. This solution predicted that test particles in the model would in general be undergoing mutual expansion or contraction.

Little attention was paid to Friedmann's evolving universe until it was independently rediscovered in 1927 by G.Lemaître. For, just two years later E.Hubble, using the 100 inch Mount Wilson telescope, reported that the spectral lines in the light from stars in 18 nearby galaxies predominately exhibited a shift in wavelength towards the red end of the spectrum. He found the farther a galaxy was from the Earth, the greater was the redshift. If λ_{ob} and λ_{em} are the observed and emitted wavelengths respectively and defining the redshift as $z \equiv (\lambda_{ob} - \lambda_{em})/\lambda_{em}$, Hubble annouced a roughly linear relationship between the distance of a galaxy and its redshift z.

The frequency shift of the stellar spectral lines had in fact been reported a number of years earlier by V.Slipher. He began a survey of spiral nubulae in 1912 and of the 41 objects he listed, 36 exhibited a redshift. However at this time it was not certain whether the nubulae were within the Milky Way or separate star systems situated beyond our galaxy. It was not until 1925 that Hubble, by measuring the apparent magnitude of variable stars of known intrinsic luminosity, established that the spiral nubulae were indeed well outside our galaxy.

Hubble, in collaboration with Humason, continued the galactic surveys into the 1930's, and extended the programme to more distant galaxies. They verified the linearity of the redshift-distance relation and by plotting cz against distance (c is the velocity of light), gave the constant of proportionality as 550 Km s^{-1} Mpc^{-1} (where 1 pc = 3·26 light years). This constant later became known as the Hubble constant H.

In 1936 Hubble, by reaching to the limit of the Mount Wilson telescope, made one of the deepest optical surveys by counting galaxies out to distances ~1000 Mpc. On these scales he found no evidence of clustering and his results provided the first clear indication that galaxies were distributed homogeniously when averaged over very large scales.

The most favoured interpretation of the cosmological redshift was, and still is, the Doppler shift caused by the motion of the distant galaxies away from the observers on Earth. This result was therefore in accordance with the Friedmann model.

The linearity of the redshift-distance relation had in fact been anticipated theoretically back in 1923 when H.Weyl, by studying a particular class of Friedmann models (the de Sitter solution), was able to show that the solution implied a linear relationship between the velocity of test particles and their mutual distance, provided the distance was small enough. E.Milne later pointed out that the linear relationship, or the Hubble law as it was subsequently called, was an immediate consequence of the homogeneity and isotropy assumptions.

The discovery of the extragalactic redshift was followed by theoretical calculations on the properties and mechanics of ever expanding and contracting Friedmann universes. These calculations focused on the problem of noninteracting and interacting matter-radiation continuum universes — the matter and radiation being smoothed out to form uniform distributions. The continuum models discussed general thermodynamic properties,and temperature and entropy variations in oscillating and ever expanding universes (Lemaître 1931; Tolman 1931, 1934). Although this approach was developed in later research (Davidson 1962; McIntosh 1968; May and McVittie 1970, 1971), with so little empirical data available these models could only supply broad insights into the properties that might be found in more realistic models.

With the completion of the 200 inch telescope at Mount Palomer in 1950 the galactic surveys were taken up again. More information could now be gained on the value

of H, and a second aim was to try and select one of the various Friedmann models as the best approximation to the observed universe.

One way of selecting between the different models was to measure the deceleration of the galactic recession owing to the galaxies mutual gravitational attraction. This deceleration is described mathematically by the parameter q, and if at the present epoch $q > \frac{1}{2}$ then the universe will eventually stop expanding and collapse back onto itself. But if $q \ll \frac{1}{2}$ then the gravitational attraction is unable to stop the galactic expansion and the universe will continue to expand indefinitely.

In 1956 Humason, Mayall, and Sandage, after an extensive survey using the 200 inch Mount Palomar telescope, gave the Hubble constant as $H \sim 180$ Km s^{-1} Mpc^{-1} and the deceleration parameter as $q \sim 3{\cdot}7$. During the following years further observations brought both H and q to lower values. In 1968 Sandage estimated that $H \sim 75$ Km s^{-1} Mpc^{-1}, and analysis by Peach in 1970 led to $q \sim 1{\cdot}5$.

Observational values of H and q have undergone much revision and are still not agreed even within a factor of two. For while the speed of galactic recession is readily measured by the redshift of the spectral lines, the determin-ation of the cosmic distance presents a more complicated problem because of the difficulty in finding reliable 'standard candles' in extragalactic objects. For example, Vaucoulers(1982) and Aaronson et al. (1980) give $H \simeq 95$ Km s^{-1} Mpc^{-1} and Kristian et al. (1978) have $q \ll 1{\cdot}6$, whereas Sandage and Tammann(1982) estimate $H \simeq 50$ Km s^{-1} Mpc^{-1} and Yahil et al. (1980) report $q < 0{\cdot}02$.

A number of surveys have taken up Hubble's 1936 programme of using galactic counts to test the assumptions of homogeneity and isotropy of the galactic distribution. A survey by Sandage et al. in 1972 assumed the universal mass density to have the distribution $\rho \propto r^{-\theta}$, where r is the distance from our locality. They found that θ does not differ significantly from zero when r is averaged over scales of ~ 100 Mpc. A study by Davis et al. (1982) suggests that galaxies supercluster (a cluster of cluster

of galaxies) up to scales ~60 Mpc. Observations by Kirshner et al. (1981) report an apparent absence of galaxies, in the direction of the Boötes constellation, over a volume corresponding roughly to a cuboid of side 100 Mpc, and measurements by Bahcall and Soneira (1982), using the Abell catalogue of galaxies, suggest a second void of similar dimensions. Although further observations have not been able to support Kirshner's results (Balzano and Weedman 1982; Sanduleak and Pesch 1982), the dimensions of the voids are still small compared to the universe as a whole and their presence would not undermine the fundamental principles of homogeneity and isotropy assumed by the standard model (Zeldovich et al. 1982).

Modern deep surveys on scales of ~1000 Mpc are still beset by the same problems as Hubble's 1936 programme of controlling the systematic errors and estimating the evolution of the distant galactic sources. A deep survey by Tyson and Jarvis (1979) suggests some deviation from homogeneity, although the size of the deviation is about what is expected before the correction for the shift of the galaxy spectrum into the red and for the allowance of cumulative errors (Peebles 1980).

The discovery of quasars and very active extragalactic radio sources provide further probes into deep space because many of these sources are thought to lie at very large distances ~3000 Mpc. Their distribution across the sky is very close to random and gives further support to the evidence that the matter distribution on large scales is very close to being homogeneous and isotropic (Fanti, Lari, and Olori 1978; Seldner and Peebles 1978).

If the matter at the present epoch is under mutual recession then an extrapolation back in time leads to the conclusion that the matter was once in a very dense state. In 1948 R.Alpher, H.Bethe, and G.Gamow considered the physics of the early stages of such a universe. They suggested that the universe was initially very hot as well as very dense and the resulting thermonuclear fusion reactions would build up simple nuclei such as deuterium and helium.

Further analysis by Alpher and Herman predicted that the radiation left over from the hot initial stages should still be present and pervade the universe as highly redshifted isotropic blackbody radiation at a temperature $\simeq 5$ K (Alpher and Herman 1950). The discovery of this microwave radiation was made in 1965 by A.Penzias and R.Wilson. They found the radiation to be highly isotropic and apparently with a blackbody distribution at a temperature $\simeq 3$ K. Recent measurements confirm the isotropy of the radiation and show that flucuations in its temperature T_r over angular scales are only $\Delta T_r/T_r < 2\times10^{-4}$ (Partridge 1980; Uson and Wilkinson 1982).

During the early universe the radiation is strongly coupled to the matter via the Compton scattering of the electrons and photons. As the matter cools on expansion, the electrons combine with the protons to form hydrogen atoms. The coupling between the hydrogen atoms and the radiation is exceedingly weak and the radiation expands essentially adiabatically under the universal expansion. The radiation temperature T_r varies inversely with the expansion factor and the high degree of isotropy of the radiation indicates that since recombination the universal expansion has been isotropic about the Earth to an accuracy of at least two parts in ten thousand.

The discovery of the background radiation was followed by more detailed calculations on the formation of elementary nuclei by using particle model universes to study the early hot stages of expansion (Peebles 1966; Wagoner, Fowler, and Hoyle 1967; Wagoner 1973). These models described the particle types and particle interactions of the matter and predicted a characteristic mass abundance M, of helium-4 $M_{He^4} \sim 20\% - 30\%$; hydrogen $M_H \sim 70\% - 80\%$; and minor traces of deuterium D, helium-3 He^3, and lithium-7 Li^7.

These predictions can be checked by observations, although an allowance must be made because the abundances at the present epoch, particularly in the vicinity of stars, may not reflect their true primordial value, as all these elements can be either created or destroyed in stellar evolution. Searle and Sargent (1972) made observations of

young, metal poor, dwarf galaxies and found that the H_e^4 mass abundance lies in the range 27% - 31%. Recent measurements of the abundances on dwarf galaxies (Olive et al. 1981; Kinman and Davidson 1982), and on Jupiter and Saturn (Gautier and Owen 1983), have brought the estimate of the primordial H_e^4 mass abundance down a little to $\sim 24\%$.

The abundance of the primordial trace elements D, H_e^3, and L_i^7, are less well known because of the uncertainty of their production and destruction during stellar nucleo--synthesis. By observing the spectral lines of interstellar material, Vidal-Majdar et al. (1977) give the present day deuterium to hydrogen mass fraction as $\sim 10^{-5}$. After making corrections for the destruction of deuterium during galactic evolution, the pregalactic deuterium mass abundance is estimated to be $M_D \simeq 5 \times 10^{-5}$ (Pagel 1982). Calculations show that the deuterium abundance produced in the early universe is very sensitive to the initial baryon density (Wagoner 1973), and an abundance this high suggests an open universe.

A present day helium-3 mass abundance $M_{H_e^3} \simeq 8 \times 10^{-5}$ has been proposed by Rood et al. (1979) by observing the emission lines in H II regions. They report that this value however, can only be an upper limit on the primordial H_e^3 abundance because H_e^3 produced by stellar nucleosynthesis could entirely swamped the cosmological contribution. An estimate of the lithium-7 abundance has been made by Spite and Spite (1982) by observing very old, metal poor, dwarf stars. They find $M_{L_i^7} \simeq 5 \times 10^{-10}$ and claim this value must be close to the pregalactic value because the destruction of the lithium has not been effective in the outer layers of these stars.

The two powerful assumptions of homogeneity and isotropy imposed on the material content of the universe are sometimes referred together as the 'cosmological principle'. Another important assumption adopted by the Friedmann model, and by most other cosmological studies, is the invariance of the physical laws governing the model. Cosmological events extend over enormous space and time scales, so do the laws of physics which are found to hold good at the present epoch and locality have universal significance ? For example, the events of the early

universe are predicted by the standard model to have occurred $\sim 10^{10}$ years ago. By extrapolating the theory back to this point we are assuming the laws of the present can be 'scaled up' and still remain applicable to such remote events in space and time. Cosmology is unlike any other branch of physics in the sense that the events it attempts to describe are unique. There is not available for study many universes whose common properties and laws can be established, but only one observable universe and study can only be made of this one single phenonena.

One way to test the invariance of the physical laws is to make a comparison between the physical constants (such as G, h, c, e, m_e), at distant spacetime points with their present day laboratory values. First, it can be asked if these fundamental constants are changing in our locality with time. Techniques such as analysis of radioactive decay, observations of planetary distances, and study of the motion of the Moon, have shown that there is little evidence of changes in the constants during the history of the Earth (Tayler 1980).

Secondly, it can be enquired if the physical constants might show variations with location from the Earth. By studying the spectral lines in quasars, objects which are thought to be very remote in space and time, Tubbs and Wolfe (1980) set stringent limits on the variation of $\alpha^2 g_p m_e / m_p$ (where α is the fine structure constant and g_p is the gyromagnetic ratio of the proton). If t_0 is the current age of the universe then they find that $\alpha^2 g_p m_e / m_p$ is spatially uniform to a few parts in 10^4 after the epoch $t \simeq 0{\cdot}05 t_0$, and they exclude time variations to the same degree of accuracy subsequent to $t \simeq 0{\cdot}20 t_0$. They conclude that for a complex quantity like $\alpha^2 g_p m_e / m_p$ to be uniform throughout most of space-time, suggests that the physical laws are indeed globally invariant.

We have seen in this section that the standard model was first proposed in the 1920's by Friedmann and Lemaître. During the following sixty years the observational

techniques have greatly improved and the empirical data have become more testing and stringent. However, the Friedmann model remains in good agreement with the observational constrainsts and it continues to be the most favoured cosmological model.

1.2 Outline of this investigation

The main objectives of this investigation are: (1) To make a further development of continuum Friedmann universes by studying the consequences of various matter-radiation interactions and how they affect the temperature and entropy changes in the model, and to discuss the connection between the interaction and the irreversibility of oscillating models. 'Heat death' characteristics (ever expanding case) are also considered (Chapter 2). (2) To devise a new model, a continuum-particle model, which can include the effects of particle interactions such as annihilation and element formation and, in addition, can incorporate the continuum interactions (Chapter 3). (3) To generalise the classical Thomson matter-radiation interaction by developing a relativistic, quantum-mechanical approach for the momentum transfer during electron-photon scattering. This leads to an expression for the momentum transfer rate between the electrons and photons which is applicable at high temperatures $T > 10^7$ K, and which predicts the well known Thomson scattering formula when temperatures are lower $T < 10^7$ K (Chapter 4).

The motivation for these objectives arises from four facts : (i) The Friedmann models are in reasonable agreement with many independent observations (see Section 1.1). (ii) Observational evidence has, so far, been unable to select between the oscillating and ever expanding solutions to describe the universe, so further discussion of both model types must be expected to remain important. (iii) Much current research combines particle physics and

cosmology and has been particulary successful in studying the early universe. However, this approach deals with short time intervals and does not in general describe persisting trends or cumulative effects over long time scales. To describe such effects and trends one has to pass from these particle models to continuum models.
(iv) In the standard model of the early universe the main thermal interaction between the matter and radiation is the classical Thomson scattering of the photons and free electrons. Many cosmological studies begin at very high temperatures when the classical approximation is no longer valid, and to find the energy transfer between the matter and radiation at these high temperatures one needs a more general, relativistic, quantum-mechanical expression for the electron-photon scattering interaction.

We have seen in Section 1.1 how the Friedmann models are still in good agreement with the observational constraints arising from the abundance of elements, the distribution and redshift of extragalactic sources, the background microwave radiation etc. Consequently a large part of cosmological research has been focused on the Friedmann solution, although the question of selecting between the open and closed models to describe the observed universe remains undecided.

The mass density of the universe measured on the scale of clusters of galaxies by inferring from the dynamical structure of the clusters, suggests an open universe (Davis et al. 1980; Symbalisty, Yang, and Schramm 1980; Press and Davis 1982), although Linscott and Erk (1980) claim there may be sufficient intergalactic material to stop the universal expansion and cause a recontraction. Luminous nucleonic matter appears incapable of accounting for the mass of clusters of galaxies (Faber and Gallanger 1979; Ford et al. 1981), and one approach has been to assume that large quantities of matter are hidden in nonluminous material, such as very cold stars, dead population III stars, black holes etc. (Gott et al. 1974; Field 1976).

Alternatively the hidden mass may lie in nonnucleonic forms. It has been proposed that relic neutrinos may solve the missing mass problem (Cowsik and McClelland 1972; Lee and Weinberg 1977). Serious consideration is being given to the existence of neutrinos with nonzero rest mass (an estimate by Lyubimov et al., 1981, has $14\,\mathrm{eV} \leqslant m_{\bar{\nu}_e} \leqslant 46\,\mathrm{eV}$), and massive neutrinos could dominate the mass density of galactic clusters should the neutrino mass be of a few tens of eV (Rephaeli 1982; Melott 1983). If neutrinos have only a small mass $m_{\nu_e} \leqslant 1{\cdot}4\,\mathrm{eV}$, then they can still dominate the universal mass density and may indeed close the universe (Schramm and Steigman 1981). Similar attention is now being given to massive gravitinos (Bond, Szalay, and Turner 1982; Weinberg 1982), photinos (Cabibbo, Farrar, and Maniani 1981; Sciama 1982), and axions (Ipser and Sikivie 1983; Stecker and Shafi 1983). Further discussion of recontrating models must be expected therefore to become more urgent.

Much of the earlier cosmological research focused on the problem of noninteracting and interacting matter-radiation continuum models and their subsequent thermodynamic predictions (Tolman 1934; Davidson 1962; May and McVittie 1970, 1971). Although these questions are still considered in later work (Park 1973; Landsberg and Park 1975; Emslie and Green 1978; Szekeres and Barnes 1979), much current research is concerned with the early evolution of the universe from its very hot and dense initial state by combining elementary particle physics with cosmology (eg., Wagoner, Fowler, and Hoyle 1967; Wagoner 1973; Olive et al. 1981; Steigman 1982). This particle approach, however, studies short time intervals and does not in general discuss trends or cumulative effects over long time scales, and may not be expected therefore to describe the evolution of the universe in all respects. To discuss and gain information on such effects and trends, one has to turn from these particle models to continuum models.

For these reasons this investigation develops a continuum-particle model (Landsberg and Reeves 1982). In accordance with the foregoing arguments, this model should be of Friedmann type, be able to take account of

the continuum interactions, and to include some nucleo-
-synthesis. The theory should be flexible enough so that both oscillating and ever expanding universes can be discussed and features which manifest themselves over long time intervals studied (the phrase 'oscillating universe' means here a universe which undergoes one or more expansions and recontractions).

The investigation begins with a further development of the continuum models (Chapter 2). The continuum theory is derived (Sections 2.1 - 2.4), and the histories of the models are traced by solving the equations numerically. The effect of interaction between matter and radiation is considered on oscillating and ever expanding universes and it is shown how the interaction affects the temperature and entropy of the model (Sections 2.5 and 2.6). The connection between the interaction and the irreversibility of an oscillating model, manifested by an increase in the total energy during the cycle, is discussed in some detail (Section 2.7). Previous studies on oscillating universes have described this asymmetry (Tolman 1934; Landsberg and Park 1975; Neugebauer and Meier 1976; Donald 1978), and by attributing this phenomena to pressure effects it is shown here for the first time how the equations can bring about a decrease in the energy of the model (Section 2.7 , and Landsberg and Reeves 1980).

Other related studies on continuum oscillating models discuss universes with noninteracting components and such models tend to be time reversible (Tolman 1934; Cohen 1967; Emslie and Green 1978). Two phase interacting models will in general be time irreversible and with entropy increase even during the contracting period (Anderson and Witting 1973; Landsberg and Park 1975), although the universes discussed by Schumacher (1964) and Schmidt (1966), which predicted an entropy decrease during contraction, are a noteworthy exception.

The continuum-particle theory is devised in Chapter 3. This model is solved numerically and expansion is begun at temperatures low enough ($T = 2 \times 10^9$ K) for the equations of the model (Sections 3.1 - 3.5) to be adequate. To approach the singularity more closely would mean taking two and three body reactions into account (for example,

$n + e^+ \leftrightarrow p + \bar{\nu}_e$, $p + e^- \leftrightarrow n + \nu_e$, $p + e^- + \bar{\nu}_e \rightarrow n$), and would detract from the basic simplicity of the theory, although in principle the theory could be extended to cover this range.

The continuum-particle model furnishes a reasonable account of the development of the universe beyond the present epoch and can therefore be taken through a (truncated) cycle in the case of an oscillating universe (Section 3.6). The model lends itself to a study of the energy and entropy changes during an oscillation and its particle features allow the helium abundance to be worked out (as a check) at the same time (Section 3.3). The helium mass abundance for this model was 27·1% (this abundance is sensitive to the initial baryon density ρ_{b0} and can be pulled down somewhat by using a lower ρ_{b0}). It is found that energy is gained during a cycle and this corresponds to an entropy generation per baryon of $6{\cdot}4 \times 10^6$ k, where k is the Boltzmann constant.

The continuum-particle model contains radiation, electron and muon neutrinos, and matter consisting of neutrons, protons, and electrons and positrons. Expansion begins with all the components in thermal equilibrium at the temperature $T = 2 \times 10^9$ K. Thereafter, the neutrinos are taken to be thermally noninteracting. The neutrinos decoupling at 2×10^9 K is below the temperature assumed in the standard calculations (for example, Peebles 1966; Wagoner, Fowler, and Hoyle 1967), which take the neutrinos to be thermally noninteracting below temperatures $\sim 5 \times 10^{10}$ K. The justification and consequences of a lower neutrino decoupling temperature are discussed and it is shown how the lower decoupling temperature leads to the new result : $T_{\nu_e} = T_{\nu_\mu} (2{\cdot}74\ \mathrm{K}) > T_r (2{\cdot}70\ \mathrm{K})$ at the present epoch (Section 3.8).

The model universes presented here, although comparatively simple, are reasonably flexible and do not require excessive computer time. The continuum models are useful in describing the general thermodynamics and cumulative effects and trends of model universes, whereas the advantage of the continuum-particle models is that they include the effects of particle interactions such as

annihilation and element formation, and in addition they can incorporate the continuum matter-radiation interactions.

Like many other cosmological models, the model universes studied here are hybrid theories in the sense that they combine the standard equations of cosmology, which take gravitation into account, with the equations of thermodynamics and statistical mechanics in which gravitation is usually ignored. For systems in which the gravitational field is important, classical thermodynamics and statistics have to be replaced by a general relativistic interpretation of thermodynamics and statistics (Tolman 1934). This investigation will not however develop this line of argument and it must suffice here to merely point out the problem. More realistic models must await further studies regarding the use of thermodynamics and statistical mechanics in the presence of strong gravitational fields.

In the early universe $z \sim 1000$, the dominant interaction between the matter and radiation is the Compton scattering of the photons and free electrons. In the classical limit, when the electron velocity is much less than the velocity of light $v << c$, and the radiation temperature $T_r < 10^7$ K, this scattering becomes the Thomson scattering process. Thomson scattering has often been included in cosmological studies by calculating the momentum transfer rate F_{Th}, from blackbody radiation to an electron (Weymann 1965; Peebles 1971). F_{Th} represents the drag force on the electron as it moves through the radiation (Thomson scattering is not, however, a true absorbtion process. Normally it refers to scattering when the incident photon energy is much less than the rest energy of the electron and with no energy exchange between the photon and electron. In line with the literature we shall nevertheless continue here to refer to F_{Th} as the 'Thomson drag'). The models presented here begin at temperatures $T > 10^7$ K, as do most cosmological models, and it is the purpose of Chapter 4 to show that at radiation temperatures $T_r > 10^7$ K and electron velocities $v \sim c$, the Thomson interaction must be generalised to take into account quantum and relativistic effects (Reeves and Landsberg 1982).

At high radiation temperatures $T_r > 10^7$ K, the scattering cross section of the electron is no longer a constant as given by the Thomson cross section σ_{Th}, but becomes dependent on the incident radiation frequency. The Klein-Nishina cross section σ_{K-N} must then be adopted. For the scattering of electrons and photons when $T_r > 10^7$ K, one needs to change to the more complicated σ_{K-N}, and for $v \sim c$ one must include the relativistic Doppler effect on the incident radiation frequency. This leads to a relativistic, quantum-mechanical expression, the 'Klein-Nishina drag' F_{K-N}, for the momentum transfer rate between the radiation and electrons (Section 4.2). At lower radiation temperatures $T_r < 10^7$ K, and slow electron velocities $v \ll c$, it is shown that F_{K-N} becomes the classical Thomson formula F_{Th} (Section 4.3).

Although it is well known that at high radiation temperatures σ_{K-N} always lies below σ_{Th} (Heitler 1954; Tucker 1975), an explicit study of the resulting decrease of the theoretical momentum transfer rate for the electron-photon scattering interaction is discussed here for the first time. The momentum transfer rate from the radiation to the electrons is worked out numerically for the cases, (i) a single electron with velocity v moving through blackbody radiation at temperature T_r (Section 4.4); (ii) an equilibrium distribution of electrons at temperature T_e interacting with blackbody radiation (Section 4.5). Graphical information is presented in each case and a comparison made with the Thomson scattering prediction.

The dependence of the Klein-Nishina F_{K-N} and Thomson F_{Th} transfer rates on the electron velocity v and and the radiation temperature T_r is discussed. It is shown (Section 4.4) that the Klein-Nishina interaction has a <u>weaker</u> dependence on T_r than the T_r^4 - law given by the Thomson interaction, but has a <u>stronger</u> dependence on v than the linear dependence of the Thomson expression.

For a distribution of electrons in thermal equilibrium with blackbody radiation $T_r = T_e \equiv T$, it is found (Section 4.5) that at temperatures $T < 10^7$ K the classical Thomson momentum transfer rate is in good agreement with the relativistic and quantum-mechanical

Klein-Nishina expression. If T is increased, then at temperatures 10^7 K < T < 5×10^9 K the Klein-Nishina interaction predicted a momentum transfer rate below the Thomson value, i.e., the electrons and radiation are more weakly coupled at these temperatures in the Klein-Nishina interaction case than in the corresponding Thomson case. However at higher temperatures T > 5×10^9 K, the Klein-Nishina expression predicted the momentum transfer rate to increase rapidly with increasing T and consequently to rise above the value predicted by the Thomson formula, i.e., the electrons and radiation are more strongly coupled at high temperatures with the Klein-Nishina interaction than with the corresponding Thomson interaction. The strong coupling at high temperatures predicted by the Klein-Nishina interaction results from the incident radiation intensity increasing rapidly in the direction opposite to the electron's motion as $v \rightarrow c$ owing to the relativistic Doppler effect.

Finally, Chapter 5 summarises the main results of the investigation and considers which parts of the work could be developed further. The Index gives a list of the symbols used in the text.

CHAPTER TWO

CONTINUUM MODELS

CONTINUUM MODELS

2.1 Introduction

The continuum models consist of uniform distributions of matter and blackbody radiation with absolute temperatures $T_m(t)$ and $T_r(t)$. Particle features such as particle types, element formation, pair creation and annihilation etc., are not considered in these models. Expansion begins with the matter and radiation in thermal equilibrium. The matter and radiation exchange energy during expansion.

2.2 Dynamical equations

For a homogeneous and isotropic universe general relativity yields the relations (see for example Misner, Thorne and Wheeler 1973),

$$\frac{2\ddot{R}}{R} + \frac{\dot{R}^2}{R^2} + \frac{Kc^2}{R^2} = -\frac{8\pi G}{c^2} p \ , \qquad (2.1)$$

$$\frac{\dot{R}^2}{R^2} + \frac{Kc^2}{R^2} = \frac{8\pi G}{3} \rho \ , \qquad (2.2)$$

where ρ is the total mass density and p is the total pressure. R is the scale factor and the notation $\dot{} \equiv d/dt$ has been adopted. G and c have their usual meanings and K is the curvature index. K can have the values $-1, 0$, and $+1$, and distinguishes between the ever expanding and oscillating models because, by equation (2.2) if $K = -1$ or 0 then $\dot{R}$ is always positive (ever expanding case), and if $K = +1$ then $\dot{R}$ becomes zero during expansion beyond which the universe contracts (model with oscillation).

Multiplying equation (2.2) by R^3 and differentiating, the left hand side is then $\dot{R}R^2$ times the left hand side of equation (2.1). Consequently

$$\frac{d}{dt}(\rho c^2 R^3) + p\frac{d}{dt}(R^3) = 0 , \qquad (2.3)$$

which expresses the constancy of the total energy in a comoving volume. Writing $U = \frac{4}{3}\pi R^3 \rho c^2$, where U is the total energy in a small comoving sphere of volume V, equations (2.2) and (2.3) become

$$\dot{R}^2 = \frac{2G}{c^2}\frac{U}{R} - Kc^2 , \qquad (2.4)$$

$$\dot{U} + 4\pi p R^2 \dot{R} = 0 . \qquad (2.5)$$

The matter and radiation components can exchange energy and this enables one to replace equation (2.5) by an equation for each component,

$$\dot{U}_i + 4\pi p_i R^2 \dot{R} = \varepsilon_i \qquad (i = m, r), \qquad (2.6)$$

where ε_i is the rate of energy transfer to the i^{th} component and satisfies

$$\varepsilon_m + \varepsilon_r = 0 . \qquad (2.7)$$

2.3 Equation of state and interaction

2.3.1 Equation of state; radiation

In addition to the dynamical equations, one needs an equation of state for each component. For blackbody radiation,

$$p_r = \frac{1}{3}\frac{U_r}{V} , \tag{2.8}$$

$$U_r = aVT_r^4 , \tag{2.9}$$

where V is the volume and a is the blackbody constant.

2.3.2 Equation of state; matter

For the equation of state for the matter one could adopt the relativistic quantum gas (see, eg., Chandrasekar 1939; Landsberg 1965). However, rather than become involved in the details and complications as to the nature of matter at high temperatures and densities, it is sufficient for the present purposes to adopt an interpolation formula (Hönl 1971). If $U_{RE} = Nmc^2$ is the total rest energy of the matter, the interpolated equation must have the accepted limiting cases;

$$p_m V = \frac{2}{3}(U_m - U_{RE}) , \quad U_m - U_{RE} \ll U_{RE} \quad \left(\begin{matrix}\text{classical}\\ \text{case}\end{matrix}\right), \tag{2.10}$$

$$p_m V = \frac{1}{3}U_m - \frac{U_{RE}^2}{2U_m} , \quad U_m \gg U_{RE} \quad \left(\begin{matrix}\text{relativistic}\\ \text{case}\end{matrix}\right) . \tag{2.11}$$

To find an interpolation between the relativistic and classical regimes, equation (2.11) is augmented by two further terms so that the pressure formula becomes an expansion in terms of U_m^{-1} :

$$p_m V = \frac{1}{3} U_m - \frac{U_{RE}^2}{2U_m} + a_1 \frac{U_{RE}^3}{U_m^2} + a_2 \frac{U_{RE}^4}{U_m^3} \quad . \qquad (2.12)$$

The coefficients a_1 and a_2 are constants and are determined by imposing the constraint that equation (2.12) must predict the classical equation (2.10) when $U_m - U_{RE} \ll U_{RE}$. In the classical regime we can write $U_m / U_{RE} = 1 + x$, where $x \ll 1$, and with this notation equation (2.12) becomes

$$p_m \frac{V}{U_{RE}} = \frac{1}{3} \frac{U_m}{U_{RE}} - \frac{1}{2} \frac{U_{RE}}{U_m} + a_1 \left(\frac{U_{RE}}{U_m} \right)^2 + a_2 \left(\frac{U_{RE}}{U_m} \right)^3$$

$$= \frac{1 + x}{3} - \frac{1}{2(1 + x)} + \frac{a_1}{(1 + x)^2} + \frac{a_2}{(1 + x)^3} \quad .$$

Neglecting x^2 terms and higher gives

$$p_m \frac{V}{U_{RE}} = -\frac{1}{6} + a_1 + a_2 + \left(\frac{5}{6} - 2a_1 - 3a_2 \right) x \, . \qquad (2.13)$$

Rewriting equation (2.10) as

$$p_m \frac{V}{U_{RE}} = \frac{2}{3} \left(\frac{U_m}{U_{RE}} - 1 \right) = \frac{2}{3} x \, , \qquad (2.14)$$

and relating equation (2.14) with (2.13), we have

$$-\frac{1}{6} + a_1 + a_2 = 0$$

$$\frac{5}{6} - 2a_1 - 3a_2 = \frac{2}{3} \ ,$$

i.e., $a_1 = 1/3$ and $a_2 = -1/6$. The interpolation formula (2.12) is then

$$p_m V = \frac{1}{3}U_m - \frac{1}{2}\frac{U_{RE}^2}{U_m} + \frac{1}{3}\frac{U_{RE}^3}{U_m^2} - \frac{1}{6}\frac{U_{RE}^4}{U_m^3} \ ,$$

or

$$p_m = \frac{1}{3}\frac{U_m}{V}\psi\left(\frac{U_m}{U_{RE}}\right) \ , \qquad (2.15)$$

where

$$\psi(y) \equiv 1 - \frac{3}{2y^2} + \frac{1}{y^3} - \frac{1}{2y^4} \ . \qquad (2.16)$$

The entropy of the matter S_m is given by

$$dS_m = \frac{1}{T_m}(dU_m + p_m dV) \ , \qquad (2.17)$$

and the matter temperature T_m is determined by

$$p_m V = NkT_m \ , \qquad (2.18)$$

where k is the Boltzmann constant and N is a constant. For the entropy of the radiation one has

$$S_r = \frac{4}{3}aVT_r^3 \ , \qquad (2.19)$$

and from equations (2.8) and (2.9), the radiation temperature satisfies

$$p_r = \frac{1}{3} a T_r^4 \ . \qquad (2.20)$$

2.3.3 Thomson interaction

The matter and radiation exchange energy via Thomson interaction. This depends on the presence of free electrons and so will be effective during the early expansion when the matter is ionised by the high temperatures. This interaction takes the form (Weymann 1965; Peebles 1971), (see p 94),

$$\varepsilon_m = A T_r^4 (T_r - T_m) \ , \qquad (2.21)$$

where A contains, amongst other constants, the number of electrons which is unspecified in the continuum models. A is therefore an arbitrary parameter (the exact expression with A defined is used in the continuum-particle model, Chapter 3 Section 3.4). The Thomson interaction (2.21) is the low temperature limit of the more general Klein-Nishina interaction (see Chapter 4, and Reeves and Landsberg 1982). The interaction (2.21) is however adequate for the present purposes.

The interval over which the Thomson interaction is effective is called the opaque period. During the expansion the energy transfer ε_m goes suddenly to zero when the electrons and protons recombine. This marks the beginning of the transparent period. In a model with oscillation the interaction is effective again during contraction

because the re-ionization of the atoms produces free electrons.

A second type of interaction is the T^4-radiation law (Landsberg and Park 1975);

$$\varepsilon_m = B \frac{U_m U_r}{V} (T_r^4 - T_m^4) \ , \qquad (2.22)$$

where B is a constant. Its effect is given here for comparison purposes (see Figures 2 and 3 below).

2.4 Reduced units and the model in numerically tractable form

To simplify the computation of the equations and to remove the constants, we take a new unit (denoted by the subscipt ru) for the scale factor R, time t, and energies U_i : R_{ru}, t_{ru}, and U_{ru} respectively. The scale factor, time and total energies are rewritten as

$$R = R_{ru} r \ , \qquad t = t_{ru} \tau \ , \qquad U_i = U_{ru} u_i \ . \qquad (2.23)$$

It is convenient to choose the units R_{ru}, t_{ru}, and U_{ru} so that

$$R_{ru}^3 = \frac{3(3Nk)^4}{4\pi a U_{ru}^3} Q^4 \ , \qquad (2.24)$$

$$t_{ru}^2 = \frac{3(3Nk)^4 c^2}{4\pi a G U_{ru}^4} Q^4 \ , \qquad (2.25)$$

where Q is a constant and

$$U_{ru} = Nmc^2 \ . \qquad (2.26)$$

2.4.1 Dynamical equations and interaction in reduced units

The main equations for calculation are the dynamical equations, the interaction and the equation of state :

$$\dot{R}^2 = \frac{2G}{c^2}\left(\frac{U_m + U_r}{R}\right) - Kc^2 \ , \qquad (2.27)$$

$$\dot{U}_i + 4\pi p_i R^2 \dot{R} = \varepsilon_i \qquad (i = m,r), \qquad (2.28)$$

$$\varepsilon_m = AT_r^4 (T_r - T_m) \ , \qquad (2.29)$$

where the matter and radiation pressures are determined by

$$p_m = \frac{1}{3}\frac{U_m}{V}\Psi\left(\frac{U_m}{U_{RE}}\right) \ , \qquad p_r = \frac{1}{3}\frac{U_r}{V} \ . \qquad (2.30)$$

With the new units (2.23), and using the notation $' \equiv d/d\tau$, equations (2.27) and (2.28) become

$$r'^2 = \frac{2GU_{ru}t_{ru}^2}{c^2 R_{ru}^3}\left(\frac{u_m + u_r}{r}\right) - \frac{Kc^2 t_{ru}^2}{R_{ru}^2} \ , \qquad (2.31)$$

$$u'_m + \frac{4}{3}\pi\frac{R_{ru}^3}{V} u_m \psi(u_m) r^2 r' = \frac{\varepsilon_m t_{ru}}{U_{ru}} \quad (i = m), \quad (2.32)$$

$$u'_r + \frac{4}{3}\pi\frac{R_{ru}^3}{V} u_r r^2 r' = -\frac{\varepsilon_m t_{ru}}{U_{ru}} \quad (i = r), \quad (2.33)$$

where $V = 4\pi R^3/3 = 4\pi R_{ru}^3 r^3/3$. The number of particles N is not yet specified for the model, and so U_{ru} , the rest energy, can be so chosen that,

$$\frac{GU_{ru} t_{ru}^2}{c^2 R_{ru}^3} = 1 \quad (2.34)$$

With the notation $I_m \equiv \varepsilon_m t_{ru} / U_{ru}$ and $C \equiv Kc^2(t_{ru}/R_{ru})^2$, equations (2.31) to (2.33) simplify to

$$r'^2 = 2\frac{u_m + u_r}{r} - C , \quad (2.35)$$

$$u'_m = -\frac{u_m \psi(u_m)}{r} r' + I_m , \quad (2.36)$$

$$u'_r = -\frac{u_r}{r} r' - I_m . \quad (2.37)$$

The 'reduced' interaction I_m is

$$I_m = \frac{\varepsilon_m t_{ru}}{U_{ru}} = A\frac{t_{ru}}{U_{ru}} T_r^4 (T_r - T_m) . \quad (2.38)$$

The matter and radiation temperature equations, (2.18) and (2.9), take the form in the new units,

$$T_m = \frac{p_m V}{Nk} = \frac{U_{ru}}{3Nk}\psi(u_m)\,u_m = \frac{mc^2}{3k}\psi(u_m)\,u_m \,, \qquad (2.39)$$

$$T_r = \left(\frac{U_r}{aV}\right)^{\frac{1}{4}} = \left(\frac{U_{ru}}{aV}\right)^{\frac{1}{4}} u_r^{\frac{1}{4}} \,. \qquad (2.40)$$

Using (2.39) and (2.40) to express T_m and T_r, the interaction (2.38) takes the form

$$I_m = A\,\frac{t_{ru}}{aV}\,u_r\left[\left(\frac{U_{ru}\,u_r}{aV}\right)^{\frac{1}{4}} - \frac{U_{ru}}{3Nk}\,\psi(u_m)\,u_m\right]$$

$$= \frac{u_r}{r^{15/4}}\left[P\,u_r^{\frac{1}{4}} - Q\,r^{\frac{3}{4}}\,u_m\,\psi(u_m)\right], \qquad (2.41)$$

where P and Q are defined as

$$P \equiv A\,\frac{t_{ru}\,U_{ru}^{\frac{1}{4}}}{(a\tfrac{4}{3}\pi R_{ru}^3)^{5/4}} \,,$$

$$Q \equiv A\,\frac{U_{ru}\,t_{ru}}{3Nka\tfrac{4}{3}\pi R_{ru}^3} \,.$$

The parameter A contains, amongst other constants, the number of electrons in the model which is not yet specified in the continuum models. A is therefore an arbitrary parameter, and so P can be chosen to

be unity, i.e., $t_{ru} = (a\frac{4}{3}\pi R_{ru}^3)^{5/4} A^{-1} U_{ru}^{-1/4}$. With this value of t_{ru}, Q becomes

$$Q = \frac{U_{ru}^{\frac{3}{4}}}{3Nk}(a\frac{4}{3}\pi R_{ru}^3)^{\frac{1}{4}} , \qquad (2.42)$$

and the interaction, equation (2.41), simplifies to

$$I_m = \frac{u_r}{r^{15/4}}\left[u_r^{\frac{1}{4}} - Q\, r^{\frac{3}{4}} u_m \Psi(u_m)\right] . \qquad (2.43)$$

The expressions for R_{ru} and t_{ru}, given by equations (2.24) and (2.25), now follow from equations (2.34) and (2.42). The model starts in thermal equil-ibrium, and hence initially $I_m = 0$. From equation (2.43) and the initial data of Table IA, one has $u_{r0}^{\frac{1}{4}} = Q\, r_0^{\frac{3}{4}} u_{m0} \Psi(u_{m0})$, i.e. $Q = 2{\cdot}208$.

2.4.2 The entropy equations in reduced units

The radiation entropy, equation (2.19), is rewritten in the new units as

$$S_r = \frac{4}{3} aVT_r^3 = \frac{4}{3} aV\left(\frac{U_r}{aV}\right)^{\frac{3}{4}}$$

$$= (a\pi)^{\frac{1}{4}}\left(\frac{4}{3}\right)^{\frac{5}{4}} (U_{ru} R_{ru})^{\frac{3}{4}} (r\, u_r)^{\frac{3}{4}} .$$

Or

$$S_r = 4QNk(r\, u_r)^{\frac{3}{4}} , \qquad (2.44)$$

where equation (2.42) has been used to replace $R_{ru}^{\frac{3}{4}}$.

With the matter temperature and pressure expressed by equations (2.39) and (2.30) respectively, the matter entropy is rewritten as

$$dS_m = \frac{1}{T_m}(dU_m + p_m dV)$$

$$= \frac{3k}{mc^2 \psi(u_m) u_m}\left[U_{ru}\, du_m + U_{ru}\, \psi(u_m)\, \frac{u_r}{r}\, dr\right].$$

With $U_{ru} = Nmc^2$ (equation (2.26)), the matter entropy becomes

$$dS_m = 3Nk\left[\frac{du_m}{\psi(u_m) u_m} + \frac{dr}{r}\right]. \qquad (2.45)$$

The total entropy S is derived from

$$dS = dS_m + dS_r .$$

The equations to solve are the three coupled differential equations (2.35) to (2.37), together with the interaction (2.43). A fourth order Runge-Kutta method (see for example Scheid 1968), was used to find a numerical solution (employing Fortran language) for r, u_m, and u_r as a function of time τ. The matter and radiation temperatures and entropies are determined throughout the model's history by equations (2.39), (2.40) and (2.44), (2.45) respectively.

2.5 Oscillating model

The earlier results (Landsberg and Park 1975) for the T^4-interaction (2.22), were confirmed by an independent calculation. When the model was run without interaction, it was established that the cycle is time symmetric about the instant of maximum expansion and has constant entropies (2.44) and (2.45). Thus, as expected, the system has no 'arrow of time', and irreversibility is due to the exchange of energy between the components.

Expansion begins with the matter and radiation in thermal equilibrium and with zero net interaction. Putting $I_m = 0$ in equation (2.43), the initial equil-ilbrium condition for the scale factor and matter and radiation energies is

$$u_{r0}^{\frac{1}{4}} = Q\, r_0^{\frac{3}{4}}\, u_{m0}\, \psi(u_{m0}) ,$$

where r_0, u_{m0}, and u_{r0} are initial values. The model has a singularity at $r = 0$ and the computation starts just away from this point at $r = 0{\cdot}27$, $u_{m0} = u_{r0} = 2{\cdot}0$, and $\tau = 0{\cdot}025$.

Figure 1 shows (in reduced units) the scale factor R, the matter-radiation temperature T_m / T_r, and entropy change S, for one cycle. During the trans-parent period, there is no energy exchange between the matter and radiation which expand adiabatically, and with no change in their entropies. On contraction T_m and T_r increase and T_m / T_r approaches unity. When $T_m / T_r \simeq 1$, the interaction I_m, equation (2.43), is small and the entropy reaches a stationary value (Figure 1). T_m / T_r then overshoots unity somewhat and the entropy shows a further increase.

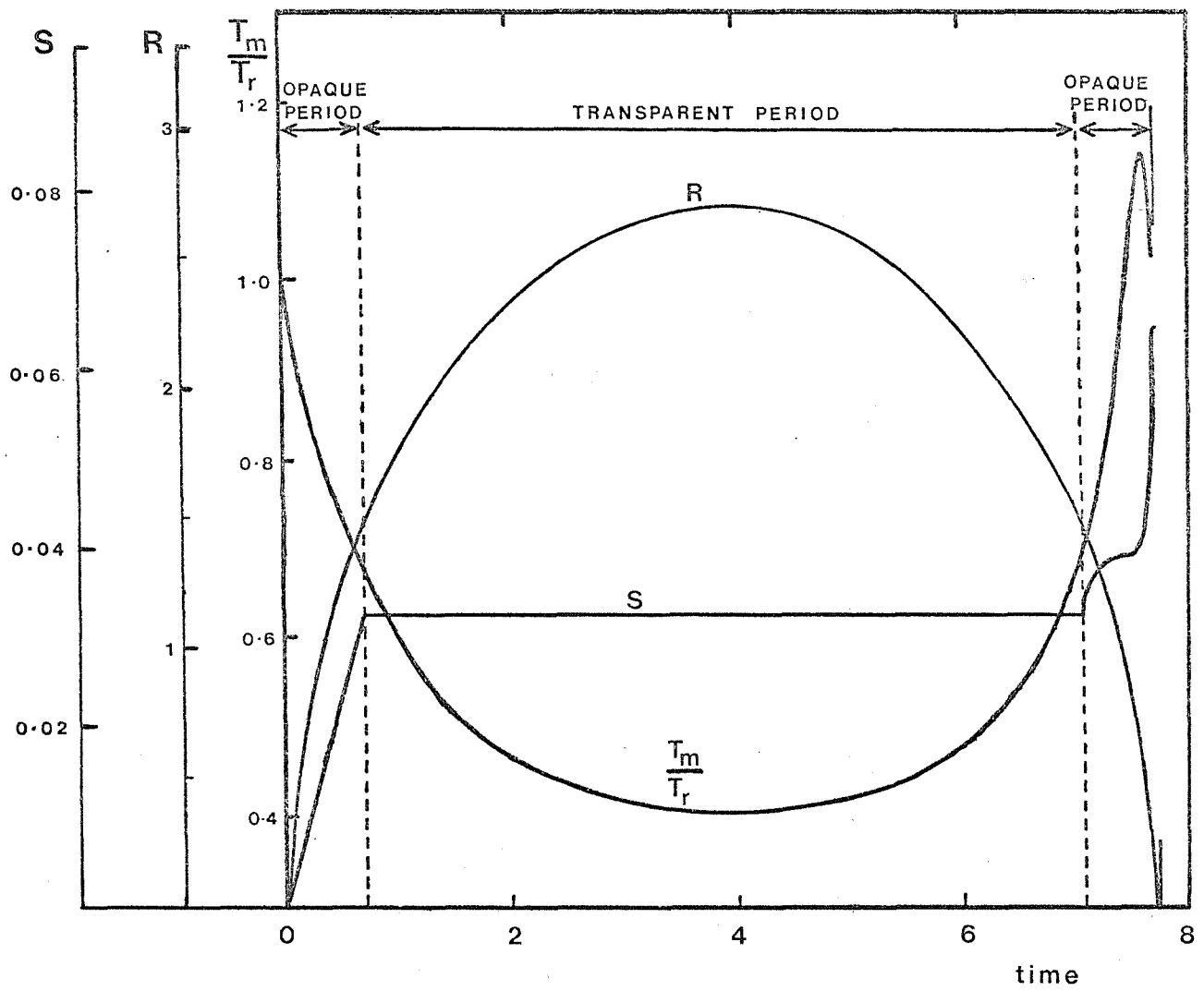

FIGURE 1 Model type : continuum, oscillating, Thomson interaction, reduced units. The figure illustrates the time dependence of the entropy S, the temperature T_m/T_r, and the scale factor R. The computed cycle time extends from $t = 0{\cdot}025$ to $t = 7{\cdot}756$.

The cycle was stopped when the scale parameter had returned to its initial value (Table IA). This value was chosen for numerical convenience and because temperatures and densities were high enough for thermal equilibrium between matter and radiation to be a good approximation. That this is so is confirmed by the closeness to equilibrium at the final cut-off. Table I gives a comparison of data for the initial and final states. Figure 1 shows that the entropy increases even in the contracting phase.

On terminating the contraction at the value of the initial scale factor one finds that there is extra energy in the final state and that the model collapses faster than its initial expansion. These results are consistent with those obtained by Landsberg and Park (1975), although the effect is larger here owing to the change in interaction from equation (2.22) to equation (2.21).

2.6 Ever expanding model

By taking a zero curvature index, $K = 0$ in equation (2.4), the models of Section 2.5 become ever expanding. Figure 2 shows the temperature difference $\Delta T = T_r - T_m$ against time for (a) T^4- interaction, (b) Thomson interaction, (c) zero interaction. Because the temperature difference ΔT is zero initially, and again after a sufficiently long period, it must have an extremum during the approach to the heat death. This feature is confirmed in Figure 2. The maximum ΔT is of course greatest in Figure 2c , and beyond the turning point a heat death develops as ΔT goes to zero. The entropy generated depends quite strongly on the chosen interaction, and there is no increase of entropy

Table I

Parameters for continuum, oscillating, Thomson scattering models near the beginning and end of an oscillation

Parameter	MODEL A			MODEL B		
	Initial state	At maximum value of R	Final state	Initial state	At maximum value of R	Final state
τ	0·025	3·891	7·756	0·025	3·818	7·611
$\dot{\tau}$	0·270	2·709	0·270	0·270	2·645	0·270
T_m	14·375	0·555	14·748	25·926	0·745	20·363
T_r	14·375	1·370	14·489	12·088	1·307	13·314
u_m	2·000	1·028	2·031	3·000	1·038	2·507
u_r	2·000	0·166	2·064	1·000	0·128	1·472
u_{tot} . . .	4·000	1·194	4·095	4·000	1·166	3·979
$\dot{\tau}$	5·361	0	-5·426	5·361	0	-5·346
S	0	0·032	0·065	0	0·965	0·157

Model A : Model with matter and radiation initially at the same temperature ($T_{m0} = T_{r0}$) in reduced units (see Section 2.4).

Model B : Model with $T_{m0} > T_{r0}$ in reduced units (see Sections 2.7 and 2.4).

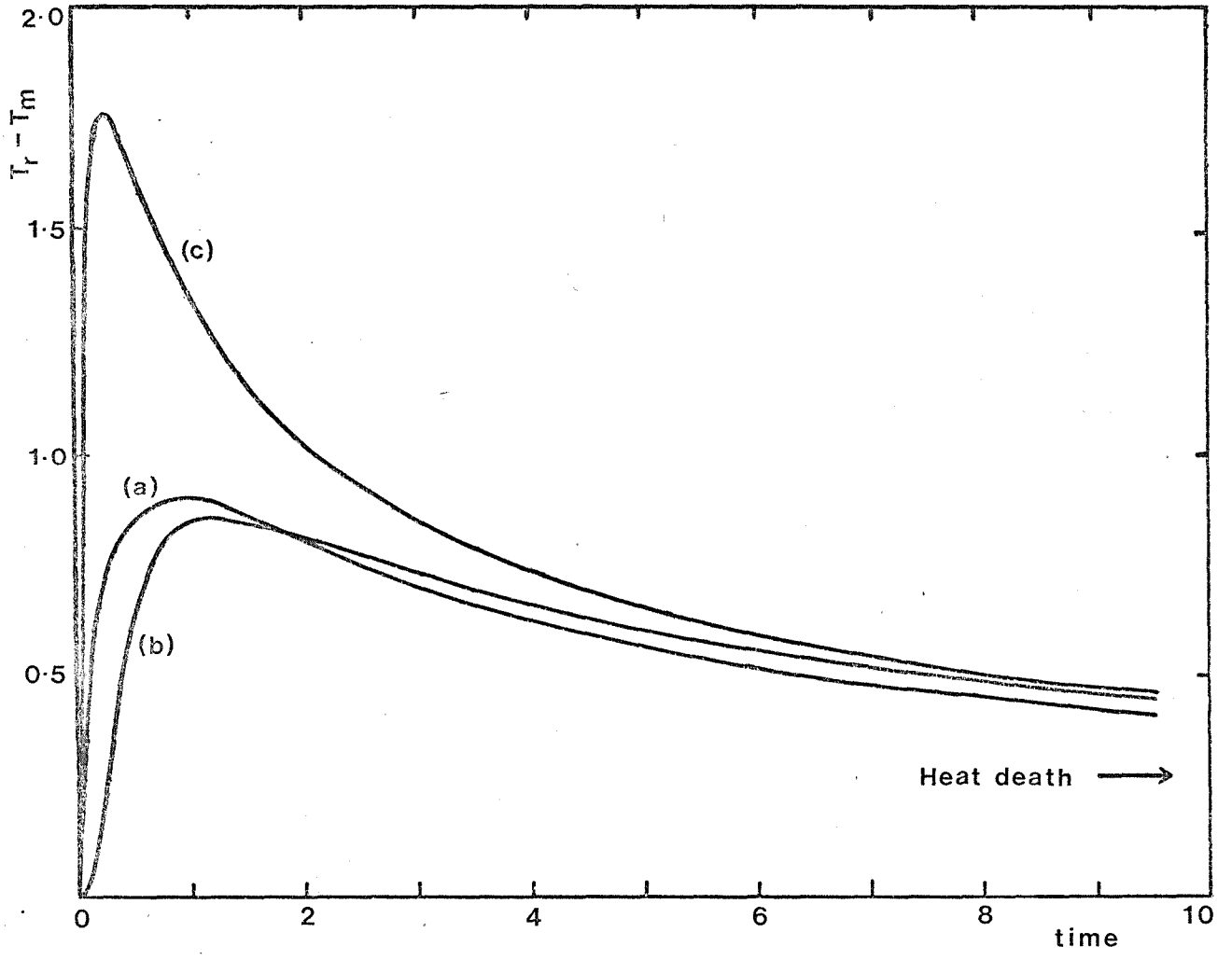

FIGURE 2 Model type : continuum, ever expanding, reduced units. The figure gives a comparison of the temperature difference $T_r - T_m$ for the cases (a) 'T^4' - interaction, (b) Thomson scattering interaction, (c) zero interaction.

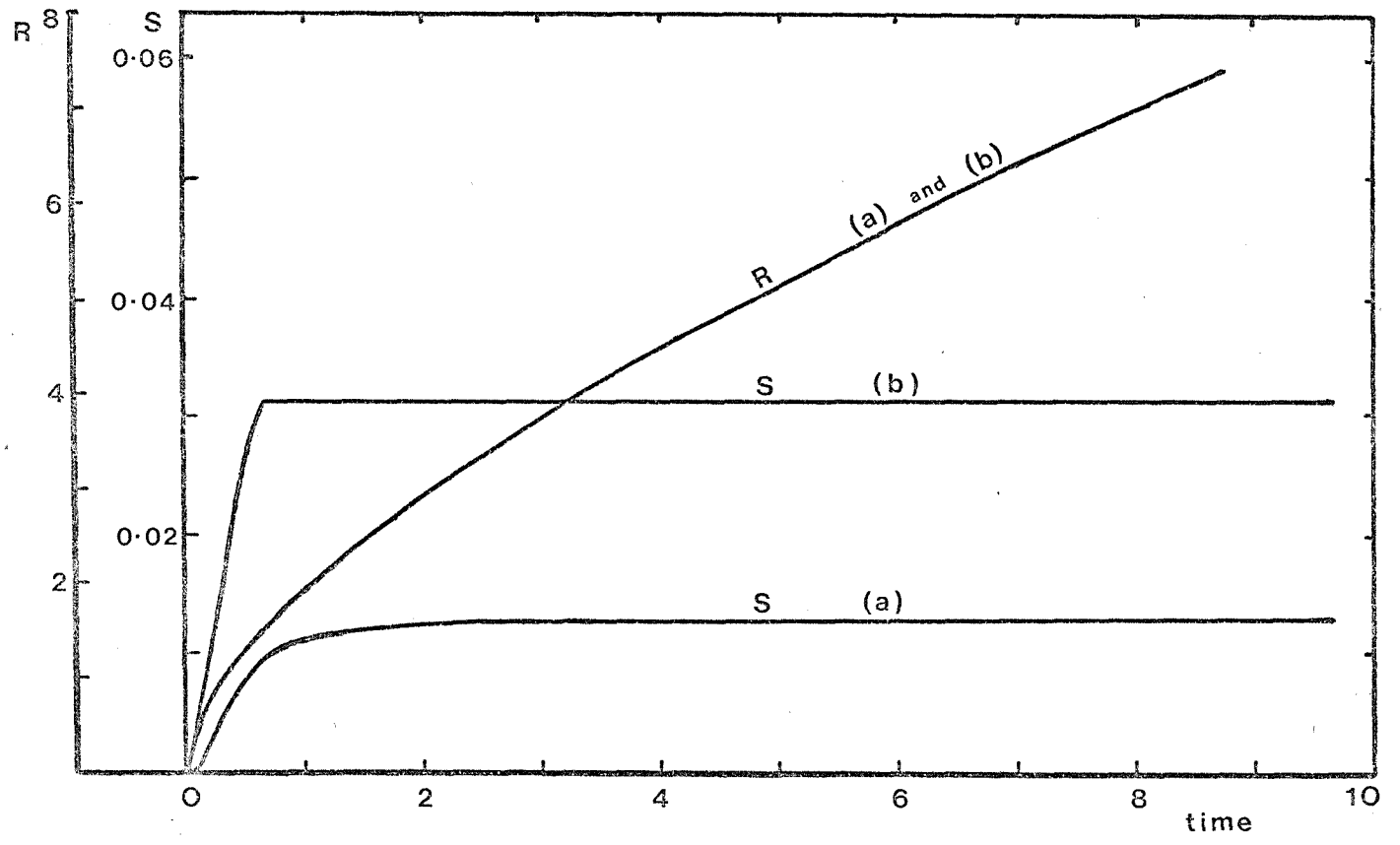

FIGURE 3 Model type : continuum, ever expanding, reduced units. The figure shows the scale factor R and entropy S for (a) 'T^4' - interaction, (b) Thomson scattering interaction.

after the interaction has ceased (Figure 3). Each case attains a time independent entropy which exceeds, or is equal to, the entropy at earlier times, as expected from thermodynamics, and confirmed in Figure 3.

2.7 Comparison of initial and final states in the continuum oscillating model

To what extent is a closed universe symmetric about its point of maximum expansion? Taking a particular element of the cosmological fluid in the expanding phase, will that same element return to an identical state when it returns to the same volume during the contracting phase?

Tolman (1934) discussed this topic qualitat-ively by using the analogy of a mixture of gases enclosed in a cyclinder with movable piston. Tolman suggested that if the gases undergo a series of expansions and contractions, then in general because of the failure to maintain equilibrium in the gas mixture and with the resulting irreversible processes taking place between the gases during the expansion, a small net amount of work will be necessary by the piston to secure a recompression to the initial volume. Tolman concluded that the entropy and energy of the gas mixture will increase after each oscillation.

Cosmological studies on oscillating universes have discussed models with noninteracting components and such models tend to be time reversible (Tolman 1934; Cohen 1967; Emslie and Green 1978). Other related studies have discussed interacting models and these are in general time irreversible and confirm Tolman's conclusions that energy and entropy increase after each oscillation (Landsberg and Park 1975; Neugbauer and Meier 1976; Donald 1978; Dicus et al. 1982; Petrosian 1982).

These conclusions are further borne out by the oscillating models discussed in Section 2.5 . By inspecting Table IA we can summarise the results as follows : On terminating the contraction at the initial scale factor one finds for the final values relative to the initial values ; (a) the energy density of both the matter and radiation has increased ; (b) the numerical value of the rate of change of the scale factor has increased ; (c) the total entropy has increased. Also we have the additional result confirmed in Section 2.5 ; (d) a noninteracting model is symmetric about the point of maximum expansion.

It is argued here that these phenomena can be attributed to pressure effects and that this interpre--tation leads one to expect opposite phenomena — lower energy and $|\dot{R}|$ - values at the cut-off scale factor than at the initial expansion corresponding to the same scale factor — if the model's pressure history is arranged appropriately (Landsberg and Reeves 1980).

The argruments involved are as follows. In noninteracting models one has $T_r \propto R$ and $T_m \propto R^{-s}$, $1 < s \leqslant 2$, while for the interacting case T_r falls more rapidly than R^{-1} and T_m more slowly than in the corresponding noninteracting case. Hence, taking an instant with the same scale factor R in an interacting and the corresponding noninteracting model, we can expect the temperatures and therefore the pressures to be different in the two models.

By checking the continuum models already discussed, which have initially $T_m = T_r$, and using the pressure equations (2.8) and (2.15), it is found that the pressure in the interacting model exceeds that for the corresponding noninteracting case. For example, writing the total pressure as $p = p_m + p_r$, then during the expanding phase of the Thomson interacting model (Section 2.5), at the 'reduced' scale factor $r = 0{\cdot}5$ the total pressure in reduced units was $p = 13{\cdot}684$, whereas the corresponding noninteracting model at the same scale

factor has $p = 13{\cdot}594$. This means that the increase in the matter pressure resulting from the interaction dominates the decrease in the radiation pressure. As a result of this greater pressure, the model does an extra amount of work compared to the noninteracting case before it arrives back at its final contraction point. The noninteracting model remains symmetric, while the extra work done by the interacting model manifests itself at that stage as extra energy in the components. If this assertion is correct then, conversely, if the pressure in the interacting model were less than in the corresponding noninteracting case, there should be less energy at the final cutt-off scale factor than was initially present in the model.

As this argument is based largely on nonrelativistic considerations, it must be checked from the relativistic equations. When this is done, it is found that by taking a model with $T_m > T_r$ initially, the drop in the matter pressure due to the interaction dominates the increase in the radiation pressure and so gives a resultant decrease in the total pressure compared to the noninteracting case. For example, for a Thomson interacting model with (in reduced units) $u_{m0} = 3{\cdot}0$, $u_{r0} = 1{\cdot}0$ and $T_{m0}(25{\cdot}93) > T_{r0}(12{\cdot}09)$ (see Table IB), then during the expanding phase at the scale factor $r = 0{\cdot}5$, the interacting model has $p = 13{\cdot}800$, while the corresponding noninteracting case has $p = 14{\cdot}333$.

The initial and final data for this model are given in Table 1B and confirm that the final total energy and rate of change of scale factor are less than their initial values. The cycle ends with the components closer to equilibrium than at the initial expansion. Although the overall energy has decreased, the entropy has still increased, in agreement with thermodynamics.

The continuum models are useful in giving the general time-dependence of thermodynamic variables, general statements about entropy changes etc., but for comparison with cosmological data, one has to turn to more realistic models. This approach is discussed in the next chapter.

CHAPTER THREE

CONTINUUM-PARTICLE MODELS

CONTINUUM-PARTICLE MODELS

3.1 Introduction

The continuum models discussed in Chapter 2 neglected the particle nature of the matter, so particle interactions such as particle creation and decay, formation of simple nuclei, etc., could not be discussed. This chapter considers a generalization of the continuum case by developing a continuum-particle theory (Landsberg and Reeves 1982). This model can incorporate the continuum interactions, and its particle features include the effects of annihilation and decay, and allow the helium abundance to be worked out at the same time. The model furnishes a reasonable account of the development of the universe up to and beyond the present epoch, can be taken through a (truncated) cycle in the case of an oscillating universe, and lends itself to a study of the energy and entropy changes during the oscillation.

The continuum-particle model is solved numeri-cally and expansion is begun at temperatures low enough ($T = 2 \times 10^9$ K) for the equations to be adequate. The disadvantage of taking only some reactions is that the detailed processes occurring near the singularity at very high temperatures ($T > 2 \times 10^9$ K) and densities cannot be discussed, and can only be included at the cost of considerable complications. This would however detract from the simplicity of the model, although in principle the theory could be extended to allow the calculation to begin closer to the singularity.

The model contains radiation, electron and muon neutrinos, and matter consisting of neutrons, protons, electrons and positrons. The electrons and positrons can annihilate and the neutrons can decay. A highly simplified

reaction network is adopted and enables one to trace the thermal history of a universe with oscillation or a universe with indefinite expansion.

3.2 Chosen initial data

The initial data is given by equations (3.1) - (3.3) and (3.5) (below), with all the components starting in thermal equilibrium. This input data is in broad agreement with the generally accepted early universe (Weinberg 1972), and corresponds to a starting time of 22·5 s after the big bang. All the variables with a subscipt 0 denote initial values and the neutron and proton components are written with a subscipt n and p, respectively. A subscipt b denotes baryons. The initial temperature, scale factor, and baryon density are

$$T_{m0} = T_{r0} = T_{\nu_e 0} = T_{\nu_\mu 0} = 2{\cdot}0 \times 10^{9}\ \mathrm{K}\,, \qquad (3.1)$$

$$R_0 = 8{\cdot}3 \times 10^{18}\ \mathrm{cm}\,, \qquad (3.2)$$

$$(\rho_n + \rho_p)_0 \equiv \rho_{b0} = 2{\cdot}40 \times 10^{-2}\ \mathrm{g\ cm^{-3}}\,. \qquad (3.3)$$

The abundance by number of a particle type i to the total number of baryons is defined by

$$X_i(t) \equiv \frac{n_i(t)}{n_b(t)}\,, \qquad (3.4)$$

where $n_i(t)$ is the number density of particles type i at

time t, and $n_b(t) = n_n(t) + n_p(t)$ is the baryon number density. The total number of baryons $N_b = n_b V$, where V is the volume, is conserved. The initial neutron number abundance is chosen to be

$$X_{n0} = 0{\cdot}1604 \qquad (3.5)$$

(Weinberg 1972). There is still some discussion of the value of the neutron half-life $t_{\frac{1}{2}}$, for the neutron decay $n \Rightarrow p + e^- + \bar{\nu}_e$. We adopt here the estimate $t_{\frac{1}{2}} = 10{\cdot}13$ minutes (Bondarenko et al. 1978).

A somewhat high initial baryon density has been chosen because this chapter concentrates on a closed, $K = +1$, model. By equations (3.4) and (3.5) the ratio of the initial neutron to proton number density is $n_{n0} / n_{p0} = 0{\cdot}1910$, and with the initial density, equation (3.3), the baryon number density is initially

$$n_{b0} = n_{n0} + n_{p0} = 2{\cdot}3011 \times 10^{21} + 1{\cdot}2045 \times 10^{22} \ \text{cm}^{-3}$$

$$= 1{\cdot}4346 \times 10^{22} \ \text{cm}^{-3} . \qquad (3.6)$$

The most nonstandard feature of the initial data is the equilibrium condition (3.1) for the neutrinos. The justification and consequences of this will be discussed in section 3.8.

3.3 The early universe

3.3.1 Neutron decay and element formation

In the early universe when temperatures and densities are too high for the nucleons to become bound into nuclei, the neutrons and protons will interchange via the weak interactions; $p + e^- \leftrightarrow n + \nu_e$, $n + e^+ \leftrightarrow p + \bar{\nu}_e$ $p + e^- + \bar{\nu}_e \leftrightarrow n$. Let r_{np} be the decay rate of a n to p (the probability per second that a neutron will decay to a proton), and let r_{pn} be the decay rate of a p to n. If $N_n(t)$ and $N_p(t)$ are the total number of neutrons and protons at time t, then the change in N_n in a time interval $t \rightarrow t + dt$ will be

$$dN_n(t) = r_{pn} N_p(t)\, dt - r_{np} N_n(t)\, dt . \qquad (3.7)$$

Dividing (3.7) by N_b and using the notation of equation (3.4), the rate of change of the neutron number abundance X_n is

$$\dot{X}_n(t) = r_{pn} X_p(t) - r_{np} X_n(t) . \qquad (3.8)$$

As the temperatures and densities fall on expansion and reach the initial values assumed here (equations (3.1) and (3.3)), the rates of the two and three body reactions becomes negligible (Weinberg 1972), and the remaining important reaction is the decay $n \rightarrow p + e^- + \bar{\nu}_e$, which proceeds at the rate of free neutron decay and must be taken into account. Equation

(3.8) simplifies to

$$\dot{X}_n(t) = -r_{np}\, X_n(t)\,, \qquad (3.9)$$

or

$$X_n(t) = N_0 \exp(-r_{np}\, t)\,, \qquad (3.10)$$

where $r_{np} = \ln 2 / 10{\cdot}13$ minutes^{-1} (Bondarenko et al. 1978). The initial data is chosen to be in general agree-ment with the standard big bang model and with the assumed initial baryon density, equation (3.3), one has $N_0 = 0{\cdot}1640$ (Weinberg 1972).

When the temperature has dropped below 10^9 K, the protons and remaining neutrons rapidly fuse into deuterium via the reaction $n + p \rightarrow D + \gamma$, and no further neutron decay takes place. The rate for the deuterium reaction is $r_D \sim 4 \times 10^{-20}\, n_b$ cm^3 s^{-1} (see for example, Wagoner, Fowler, and Hoyle 1967), where n_b is the baryon number density. During the element formation period $n_b \sim 5 \times 10^{21}$ cm^{-3}, so one has $r_D \sim 200$ s^{-1} during this period.

The universal expansion rate is $H = \dot{R} / R$, where R is the scale factor and H is Hubble's constant. At the time of element formation we have $H \sim 5 \times 10^{-3}$ s^{-1}, which is considerably slower than the deuterium reaction rate r_D. The deuterium reaction will therefore proceed much faster than the universal expansion and to a good approximation the deuterium abundance will relax to an equilibrium, Fermi distribution. For a general element type i and nuclear mass m_i, this distribution takes the form

$$n_i(q) = g_i \frac{4\pi}{h^3}\, q^2\, dq \left[\exp\left(\frac{E_i(q) - \mu_i}{kT_m} \right) + 1 \right]^{-1}, \qquad (3.11)$$

where n_i is the number density of the particles type i in

a momentum range $q \rightarrow q + dq$, $E_i(q)$ is the total energy of one particle, μ_i its chemical potential, and g_i the number of spin states.

The nucleons are nonrelativistic at the temperatures treated here and at reasonably low densities, so equation (3.11) can be approximated by the Boltzmann distribution and one can write the total particle energy as $E_i(q) = m_i c^2 + q^2/2m_i$. The particle number density n_i then becomes

$$n_i(q) = g_i \frac{4\pi}{h^3} q^2 dq \exp\left(\frac{-m_i c^2 + \mu_i}{kT_m}\right) \exp\left(\frac{-q^2}{2m_i kT_m}\right). \qquad (3.12)$$

If the temperature is too high the nuclei will be broken up just as quickly as they form, but as the temperature continues to fall on expansion the abundance of the element type i is found to rapidly rise from zero to its final value at a temperature T_f^i, called the 'freezing-in' temperature for the element type i.

To calculate T_f^i, equation (3.12) is integrated over momentum to find the number density n_i at a general temperature T_m. To proceed with the integration, the following recurrence relation proves useful,

$$I(s) \equiv \int_0^\infty e^{-ax^2} x^s dx = -\frac{\partial}{\partial a} I(s-2) \qquad s \geqslant 0 .$$

Writing $y \equiv a^{\frac{1}{2}} x$, then for $I(0)$ one has

$$I(0) = \frac{1}{a^{\frac{1}{2}}} \int_0^\infty e^{-y^2} dy ,$$

i.e.,

$$I(0) = \frac{1}{2a^{\frac{1}{2}}} \pi^{\frac{1}{2}} ,$$

(see for example Abramowitz and Stegun 1972, p302). I(2) then yields

$$I(2) = -\frac{\partial}{\partial a} I(0) = \frac{\pi^{\frac{1}{2}}}{4} a^{-3/2} . \qquad (3.13)$$

Now writing $a \equiv (2m_i kT_m)^{-1}$ and using the result (3.13), the integration of equation (3.12) over all momenta gives

$$n_i = g_i \frac{4\pi}{h^3} \exp\left(\frac{-m_i c^2 + \mu_i}{kT_m}\right) \frac{\pi^{\frac{1}{2}}}{4} (2m_i kT_m)^{3/2}$$

$$= g_i \left(\frac{2\pi m_i kT_m}{h^2}\right)^{3/2} \exp\left(\frac{-m_i c^2 + \mu_i}{kT_m}\right) . \qquad (3.14)$$

Let A_i be the nucleon number and P_i the proton number for the element type i, then each nucleus contains $A_i - P_i$ neutrons. The neutrons and protons have nearly equal mass, so to a good approximation the abundance by mass of the element i to all baryons is

$$M_i = A_i \frac{n_i}{n_b} , \qquad (3.15)$$

where n_b is the number density of all baryons (bound plus free baryons). Let n_n and n_p be the number density of the <u>free</u> neutrons and <u>free</u> protons respectively, then the abundance by mass of the free neutrons and free protons

to all baryons is just $M_n = n_n/n_b$ and $M_p = n_p/n_b$ respec-
-tively. n_n and n_p can be introduced into the equation (with the view that the chemical potentials μ_i, μ_n, μ_p, will later cancell out), by rewriting (3.15) as a relation between M_i, M_n, and M_p:

$$M_i = A_i \frac{n_i}{n_b} \left(\frac{n_b}{n_n}\right)^{A_i - P_i} M_n^{A_i - P_i} \left(\frac{n_b}{n_p}\right)^{P_i} M_p^{P_i} . \qquad (3.16)$$

Substituting the number density equation (3.14) into the mass abundance equation (3.16), one has

$$M_i = A_i g_i \left(\frac{2\pi m_i kT_m}{h^2}\right)^{\frac{3}{2}} \exp\left(\frac{-m_i c^2 + \mu_i}{kT_m}\right) n_b^{A_i - 1} \left(\frac{M_n}{n_n}\right)^{A_i - P_i} \left(\frac{M_p}{n_p}\right)^{P_i} . \qquad (3.17)$$

The number density of free neutrons and free protons, n_n and n_p, is determined by equation (3.14) with $i = n$ and $i = p$, respectively, and with $g_n = g_p = 2$. Substituting the expressions for n_n and n_p into equation (3.17), and using the approximations $m_n = m_p \equiv m_b$ and $m_i = A_i m_b$ in the 3/2 power term only, yields

$$M_i = \frac{A_i g_i \left(\frac{2\pi A_i m_b kT_m}{h^2}\right)^{\frac{3}{2}} \exp\left(\frac{-m_i c^2 + \mu_i}{kT_m}\right) n_b^{A_i - 1} M_n^{A_i - P_i} M_n^{P_i}}{2^{A_i} \left(\frac{2\pi m_b kT_m}{h^2}\right)^{\frac{3A_i}{2}} \exp\left[\left(\frac{-m_n c^2 + \mu_n}{kT_m}\right)(A_i - P_i)\right] \exp\left[\left(\frac{-m_p c^2 + \mu_p}{kT_m}\right) P_i\right]} . \qquad (3.18)$$

The chemical potential μ_i is conserved in the reactions so μ_i can be written as a sum of the neutron and proton chemical potentials; $\mu_i = P_i\mu_p + (A_i - P_i)\mu_n$. Now substituting μ_i into equation (3.18), the mass abundance M_i becomes after some cancellation,

$$M_i = \frac{A_i^{\frac{5}{2}} g_i}{2^{A_i}} \frac{n_b^{A_i-1} M_n^{A_i-P_i} M_p^{P_i}}{\left(\frac{2\pi m_b kT_m}{h^2}\right)^{\frac{3}{2}(A_i-1)}} \exp\left[\frac{-m_i c^2 + m_n c^2(A_i - P_i) + m_p c^2 P_i}{kT_m}\right]$$

$$= \frac{A_i^{\frac{5}{2}} g_i}{2} M_n^{A_i-P_i} M_p^{P_i} w^{A_i-1} \exp\left(\frac{BE_i}{kT_m}\right) , \qquad (3.19)$$

where $BE_i = -m_i c^2 + m_n c^2(A_i - P_i) + m_p c^2 P_i$ is the binding energy of the nucleus of species i, and w is defined as

$$w = \frac{n_b h^3}{2} \frac{1}{(2\pi m_b k)^{3/2}} \frac{1}{T_m^{3/2}} . \qquad (3.20)$$

The coefficient $\frac{1}{2} A_i^{\frac{5}{2}} g_i M_n^{A_i-P_i} M_p^{P_i}$ in equation (3.19), is of order unity because all its terms are either just greater than or just less than one. The dominant terms in (3.19) are the exponential term and w^{A_i-1}. At large matter temperatures T_m, M_i will be very small, but M_i will rise rapidly as T_m decreases on expansion. The mass abundance of an element i will become large in

comparison to the mass of all baryons when M_i approaches unity, i.e.,

$$w^{1-A_i} = \exp\left(\frac{BE_i}{kT_m}\right) . \qquad (3.21)$$

w is very small during the element formation period, and equation (3.21) is satisfied when the matter temperature T_m has fallen to the value T_f^i, where

$$T_f^i = \frac{BE_i}{(A_i - 1)k\,|\ln w|} .$$

T_f^i is called the 'freezing-in' temperature for the element type i.

The temperature at which deuterium, $i = D$, with nucleon number $A_D = 2$ and binding energy $BE_D = 2{\cdot}22$ MeV, 'freezes-in' will be

$$T_f^D = \frac{2{\cdot}22 \text{ MeV}}{k\,|\ln w|} . \qquad (3.22)$$

At T_f^D the neutrons become bound into deuterium atoms and the neutrons no longer undergo decay.

The 'freezing-in' temperature for helium-4, H_e^4, of binding energy 28·3 MeV, is

$$T_f^{H_e^4} = \frac{28{\cdot}3 \text{ MeV}}{3k\,|\ln w|} . \qquad (3.23)$$

Because the H_e^4 nuclei have a greater binding energy than

deuterium, the deuterium atoms and remaining protons will become rapidly incorporated into H_e^4 via a sequence of reactions like $D + p \rightarrow H_e^3 + \gamma$, $D + D \rightarrow H_e^3 + n$, $H_e^3 + n \rightarrow H_e^4 + \gamma$, $D + D \rightarrow H_e^4 + \gamma$, and it is assumed that all the deuterium atoms at the deuterium freezing-in time t_f^D form into helium.

Although the freezing-in temperature for H_e^4, equation (3.23), is higher than the freezing-in temperature for deuterium, equation (3.22), the helium cannot form before deuterium because the temperatures and densities are too low for the occurrence of the required many body reactions, for example $n + p + n + p \rightarrow H_e^4$ (Weinberg 1972). Hence the final helium-4 abundance will be

$$2X_n \text{ at } t_f^D = \text{abundance by mass of } H_e^4 \text{ after } t_f^D .$$

A H_e^4 abundance of 27·1% by mass is found (this abundance is sensitive to ϱ_{b0} and can be pulled down somewhat by using a lower initial baryon density). The freezing-in time and temperature are respectively 2·8 minutes and $8{\cdot}7 \times 10^8$ K.

3.3.2 Electron-positron pairs

During the early universe the high energy radiation creates electron-positron pairs. As the matter cools on expansion, the pairs will annihilate into photons, feeding energy into the radiation component. For an oscillating model the reverse process occurs on contraction. The number density of electrons plus positrons bound in

pairs n_{ep}, is given by

$$n_{ep}(Tm) = b\,T_m^{\frac{3}{2}} \exp\left(\frac{-m_e c^2}{kT_m}\right), \qquad (3.24)$$

where m_e is the mass of an e^- or e^+, and

$$b \equiv \left(\frac{2\frac{5}{3}\pi m_e k}{h^2}\right)^{\frac{3}{2}} = 4{\cdot}829 \times 10^{15}\ \mathrm{cm}^{-3}\ \mathrm{K}^{-3/2}\ .$$

Equation (3.24) is a classical equilibrium distribution (see eg., Tolman 1934), and holds as long as $m_e c^2 > kT_m$. This distribution is justified because during the early stages of expansion thermal equilibrium is maintained between the matter and radiation by the Thomson interaction (discussed in Section 3.4), and by equation (3.1) we have initially $m_e c^2 / kT_m = 2{\cdot}97$. Putting $T_m = T_{m0}$ in equation (3.24), the initial number density of electrons plus positrons bound in pairs is

$$n_{ep0} = 2{\cdot}227 \times 10^{28}\ \mathrm{cm}^{-3}\ ,$$

or

$$\rho_{ep0} = 20{\cdot}29\ \mathrm{g\ cm}^{-3}\ . \qquad (3.25)$$

To ensure charge neutrality in the model there must be an additional number of electrons n_{ed}, equal to the initial number density of protons n_{p0}. At time t and temperature T_m, the <u>total</u> number density of electrons plus positrons n_e, will be

$$n_e(T_m, t) = n_{ep}(T_m) + n_{ed} + n_e^{decay}(t)\ , \qquad (3.26)$$

where $n_{ed} = n_{p0}$, and $n_e^{decay}(t)$ is the number density of electrons released from the neutron decay $n \rightarrow p + e^- + \bar{\nu}_e$ at time t .

The initial photon and neutrino mass densities are

$$\rho_{r0} = \frac{aT_{r0}^4}{c^2} = 134{\cdot}7 \text{ g cm}^{-3} . \qquad (3.27)$$

$$\rho_{\nu_{e0}} = \rho_{\bar{\nu}_{e0}} = \rho_{\nu_{\mu 0}} = \rho_{\bar{\nu}_{\mu 0}} = \frac{7}{16}\frac{aT_{\nu 0}^4}{c^2} = 58{\cdot}93 \text{ g cm}^{-3} . \qquad (3.28)$$

By comparing equations (3.3), (3.25), (3.27) and (3.28) one has $\rho_{r0} > \rho_{\nu_{e0}} > \rho_{ep0} > \rho_{b0}$, hence model is initially radiation dominated. Using equation (2.19) to give the radiation entropy, the initial radiation entropy per baryon η, is

$$\eta = \frac{4}{3}\frac{aT_{r0}^3}{n_{b0}} = 5{\cdot}624 \times 10^{-9} \text{ erg K}^{-1}$$

$$= 4{\cdot}074 \times 10^7 \text{ k} ,$$

where k is the Boltzmann constant.

3.4 Equation of state and interaction

3.4.1 Equation of state ; matter

In the continuum-particle model expansion begins at a temperature 2×10^9 K and with the matter semi-relativistic. The equation of state for the matter must be expected therefore to take into account special relativistic effects, and to express the total energy of the matter U_m, as a function of the matter temperature T_m.

In order to relate U_m and T_m one could adopt the full relativistic-quantum gas (see for example Chrandrasekhar 1939). However this would add considerable complications to the model because of the integrals which occur, and at the temperatures and densities treated here it is sufficient for our purposes to adopt an approximate series expansion for U_m in terms of T_m (Hönl 1971).

The Gibbs canonical probability distribution P_j, gives the expectation value of the total energy of a perfect gas of N particles as (see for example Baierlein 1971; Landsberg 1978),

$$\langle U_m \rangle = N \sum_j E_j P_j$$

$$= \frac{N \sum_j E_j e^{-E_j / kT_m}}{\sum_j e^{-E_j / kT_m}} , \qquad (3.29)$$

where P_j is the probability that the particle is in the eigenstate ψ_j with the eigenvalue E_j. The summation j is over all eigenstates ψ_j.

Let $\underline{r}$ and $\underline{p}$ signify the position and momentum of a particle, and replacing the summation over all eigenstates by an integration over phase space, equation (3.29) becomes

$$\langle U_m \rangle = \frac{N \int_{\substack{\text{phase}\\\text{space}}} E(\underline{r}, \underline{p})\, e^{-E(\underline{r}, \underline{p})/kT_m} \frac{d^3\underline{r}\, d^3\underline{p}}{h^3}}{\int_{\substack{\text{phase}\\\text{space}}} e^{-E(\underline{r},\underline{p})/kT_m} \frac{d^3\underline{r}\, d^3\underline{p}}{h^3}}, \tag{3.30}$$

where h is the planck constant and h^3 is the volume occupied in phase space by each state. $d^3\underline{r}\, d^3\underline{p}$ is the infinitesimal volume in phase space in which the particle's position is within the region $d^3\underline{r} \equiv dxdydz$ around the position $\underline{r}$, and that its momentum is within a region $d^3\underline{p} \equiv dp_x dp_y dp_z$ around the value $\underline{p}$.

The energy of the particles in the gas will in general be dependent only on the magnitude of their momentum and not on their position and direction of motion. For a fixed magnitude of the momentum, equation (3.30) yields an integration over all directions. For an infinitesimal momentum range $p \rightarrow p + dp$, an integration over a thin spherical shell of radius p and thickness dp yields a volume $4\pi p^2 dp$. Equation (3.30) simplifies to

$$\langle U_m \rangle = \frac{N \int_0^\infty E(p)\, e^{-E(p)/kT_m}\, p^2\, dp}{\int_0^\infty e^{-E(p)/kT_m}\, p^2 dp}. \tag{3.31}$$

Special relativity gives the connection between the total energy E, and momentum p, of a particle of rest mass m_0, as

$$E^2 = c^2 p^2 + (m_0 c^2)^2 , \qquad (3.32)$$

where c is the velocity of light. Using the notation $\mathcal{E} \equiv E/m_0c^2$ and $a \equiv m_0c^2/kT_m$, $\langle U_m \rangle$ becomes

$$\langle U_m \rangle = \frac{Nm_0c^2 \int_1^\infty \mathcal{E}\, e^{-a\mathcal{E}} (m_0c^2)^3 c^{-2} (\mathcal{E}^2 - 1)^{\frac{1}{2}} \mathcal{E}\, d\mathcal{E}}{\int_1^\infty e^{-a\mathcal{E}} (m_0c^2)^3 c^{-2} (\mathcal{E}^2 - 1)^{\frac{1}{2}} \mathcal{E}\, d\mathcal{E}}$$

$$= \frac{Nm_0c^2 \int_1^\infty \mathcal{E}^2 (\mathcal{E}^2 - 1)^{\frac{1}{2}} e^{-a\mathcal{E}}\, d\mathcal{E}}{\int_1^\infty \mathcal{E} (\mathcal{E}^2 - 1)^{\frac{1}{2}} e^{-a\mathcal{E}}\, d\mathcal{E}} . \qquad (3.33)$$

Defining

$$Y \equiv \int_1^\infty \mathcal{E} (\mathcal{E}^2 - 1)^{\frac{1}{2}} e^{-a\mathcal{E}}\, d\mathcal{E} , \qquad (3.34)$$

(Y may be soluble by using Bessel functions).
equation (3.33) can be rewritten as

$$\langle U_m \rangle = Nm_0c^2 \left(-\frac{1}{Y} \frac{\partial Y}{\partial a} \right)$$

$$= -Nm_0c^2 \frac{\partial}{\partial a} (\ln Y) . \qquad (3.35)$$

Expanding the square root in the integrand of equation (3.34) in declining powers of ε (note $\varepsilon > 1$), one has

$$Y = \int_1^{\infty} \left(\varepsilon^2 e^{-a\varepsilon} - \frac{e^{-a\varepsilon}}{2} - \frac{e^{-a\varepsilon}}{8\varepsilon^2} - \frac{e^{-a\varepsilon}}{16\varepsilon^4} - \ldots . \right) d\varepsilon . \quad (3.36)$$

The integration of the first term in (3.36) can be simplified by integration by parts. Thus,

$$\int \varepsilon^2 e^{-a\varepsilon} d\varepsilon = \int \varepsilon^2 \frac{d(e^{-a\varepsilon})}{-a}$$

$$= - \frac{\varepsilon^2 e^{-a\varepsilon}}{a} + \frac{2}{a} \int \varepsilon e^{-a\varepsilon} d\varepsilon$$

$$= - e^{-a\varepsilon} \left(\frac{\varepsilon^2}{a} + \frac{2\varepsilon}{a^2} + \frac{2}{a^3} \right) . \quad (3.37)$$

The third and fourth terms in the integrand of equation (3.36) can be neglected in comparison to the first and second terms because, for small ε the third and fourth terms are less than one, and for large ε they become vanishingly small (Abramowitz and Stegun 1972, p228).

With the third and fourth terms neglected and with the result (3.37), equation (3.36) gives after integration,

$$Y = e^{-a} \left(\frac{1}{a} + \frac{2}{a^2} + \frac{2}{a^3} \right) - \frac{e^{-a}}{2a}$$

$$= e^{-a} \left(\frac{1}{2a} + \frac{2}{a^2} + \frac{2}{a^3} \right) . \quad (3.38)$$

Substituting (3.38) back into equation (3.35), the total energy of the gas becomes

$$U_m = -Nm_0c^2 \frac{\partial}{\partial a}\left[\ln\left(\frac{2}{a^3} + \frac{2}{a^2} + \frac{1}{2a}\right) - a\right]$$

$$= Nm_0c^2\left[\frac{6 + 4a + \frac{1}{2}a^2}{2a + 2a^2 + \frac{1}{2}a^3} + 1\right].$$

Summing over all particle types i, and introducing the temperature dependence, the equation of state for the matter becomes

$$U_m(T_m) = \sum_i N_i m_i c^2\left[\frac{6 + 4a_i(T_m) + \frac{1}{2}a_i^2(T_m)}{2a_i(T_m) + 2a_i^2(T_m) + \frac{1}{2}a_i^3(T_m)} + 1\right], \tag{3.39}$$

where $i = n,p,e$ denotes the neutrons, protons, and electrons plus positrons, and $a_i(T_m) \equiv m_i c^2/kT_m$.

The equation of state (3.39), can be checked for extrapolation by taking the two extreme cases $a_i \ll 1$ (relativistic) and $a_i \gg 1$ (classical). Expanding the denominator of (3.39) first in increasing powers of a_i for the relativistic case, and then in increasing powers of a_i^{-1} for the classical case, we have respectively

$$U_m = \sum_i N_i m_i c^2\left[(6 + 4a_i + \frac{1}{2}a_i^2)\left(\frac{1}{2a_i} - \frac{1}{2} + \frac{3}{8}a_i + \cdots\right) + 1\right] \quad a_i \ll 1,$$

$$U_m = \sum_i N_i m_i c^2\left[(6 + 4a_i + \frac{1}{2}a_i^2)\left(\frac{2}{a_i^3} - \frac{8}{a_i^4} + \frac{24}{a_i^5} + \cdots\right) + 1\right] \quad a_i \gg 1.$$

Neglecting a_i^2 terms and higher for the case $a_i \ll 1$, and a_i^{-2} terms and lower when $a_i \gg 1$, the matter energy U_m has the accepted limiting cases

$$U_m = \sum_i \left[3N_i kT_m + \frac{N_i (m_i c^2)^2}{2kT_m} \right] \qquad kT_m \gg m_i c^2 ,$$

$$U_m = \sum_i \left[N_i m_i c^2 + N_i kT_m \right] \qquad kT_m \ll m_i c^2 .$$

The dependence of the matter pressure p_m on the total energy U_m, is given by the interpolation formula (see Section 2.3.2, equation (2.15)) as,

$$p_m = \frac{1}{3} \frac{U_m}{V} \psi\left(\frac{U_m}{U_{RE}}\right) , \qquad (3.40)$$

where

$$\psi(y) \equiv 1 - \frac{3}{2y^2} + \frac{1}{y^3} - \frac{1}{2y^4} ,$$

and $U_{RE} = \sum_i N_i m_i c^2$ is the total rest energy of the matter.

3.4.2 Equation of state ; photons and neutrinos

The photon and neutrino total energies and pressures as a function of their temperatures are,

$$U_r = \rho_r c^2 V = aT_r^4 V , \qquad p_r = \frac{1}{3} aT_r^4 . \qquad (3.41)$$

$$U_\nu = \rho_\nu c^2 V = \sum_j \rho_j c^2 V = \sum_j \frac{7}{16} aT_j^4 V , \qquad p_\nu = \sum_j \frac{7}{48} aT_j^4 , \qquad (3.42)$$

where a is the blackbody constant and $j = \nu_e , \bar{\nu}_e , \nu_\mu , \bar{\nu}_\mu$ denotes the four neutrino types.

3.4.3 Thomson interaction

The temperature dependence of the Thomson interaction was introduced in Section 2.3.3, equation (2.21), for the continuum models. With the constants explicity shown the Thomson interaction takes the form (Weymann 1965; Peebles 1971),

$$\varepsilon_m = \frac{4\sigma_{Th} akN_e}{m_e c} T_r^4 (T_r - T_m) , \qquad (3.43)$$

where ε_m is the rate of energy transfer between the matter and radiation. σ_{Th} is the Thomson scattering cross section and has the value $6{\cdot}625 \times 10^{-25}$ cm^2. N_e is the total number of electrons plus positrons, and m_e is the rest mass of an electron or positron.

3.5 Dynamical equations

The continuum-particle model is governed by the dynamical equations (2.4) and (2.6). They are modified by the following : (i) a noninteracting neutrino sea giving an extra component $i = \nu$, in equation (2.6). (ii) The addition of the neutrino total energy in equation (2.6). (iii) The inclusion of the energy production rate in equation (2.6) for $i = r$, due to the e^-e^+ annihilation $d(E_e N_{ep})/dt$, where E_e is the total energy of an e^- or e^+, and N_{ep} is the total number of electrons plus positrons bound in pairs. With these modifications the dynamical equations for the scale factor R, matter energy U_m, radiation energy U_r, and neutrino energy U_ν become

$$\dot{R}^2 = \frac{2G}{c^2}\frac{U_m + U_r + U_\nu}{R} - Kc^2 \qquad (3.44)$$

$$\dot{U}_m + 4\pi p_m R^2 \dot{R} = \varepsilon_m \qquad (3.45)$$

$$\dot{U}_r + 4\pi p_r R^2 \dot{R} = -\varepsilon_m - (E_e \dot{N}_{ep} + \dot{E}_e N_{ep}) \qquad (3.46)$$

$$\dot{U}_\nu + 4\pi p_\nu R^2 \dot{R} = 0 . \qquad (3.47)$$

During expansion the e^-e^+ annihilate and the energy from the annihilation is fed into the radiation component. In a model with oscillation the reverse process occurs on contraction. The number of particles of type i, N_i, is a function of time because the electrons and positrons annihilate and the neutrons decay. The rate of change of the electron-positron pair number density, $\dot{n}_{ep}$, is given by the differential of equation (3.24), and the

rate of change of the neutron number abundance $\dot{X}_n$, is determined by equation (3.9).

The equation of state for matter (3.39), expresses the matter energy U_m as a function of matter temperature T_m. The dynamical equation (3.45) can therefore be written as a differential equation in T_m rather than U_m. Using the notation

$$f_i(T_m) \equiv \left[\frac{6 + 4a_i(T_m) + \frac{1}{2}a_i^2(T_m)}{2a_i(T_m) + 2a_i^2(T_m) + \frac{1}{2}a_i^3(T_m)} + 1 \right],$$

the total matter energy U_m, expressed as a function of temperature T_m becomes

$$U_m(T_m, t) = \sum_i N_i(T_m, t)\, m_i c^2 f_i(T_m) , \qquad (3.48)$$

where $i = n,p,e$ denotes neutrons, protons, and electrons plus positrons, and as previous $a_i(T_m) \equiv m_i c^2/kT_m$. With this notation the total energy of a paticle type i is $E_i(T_m) = m_i c^2 f_i(T_m)$. Differentiating equation (3.48) to find $\dot{U}_m$ yields

$$\dot{U}_m(T_m,t) = \sum_{i=n,p,e} \left[\dot{N}_i(T_m,t) m_i c^2 f_i(T_m) + N_i(T_m,t) m_i c^2 \dot{f}_i(T_m) \right] .$$

Writing the summation out in full and noting that the expressions f_i are explicit functions of temperature only, and N_n and N_p are functions of time only, one has

$$\dot{U}_m(T_m,t) = m_n c^2\left[\dot{N}_n(t)\, f_n(T_m) + N_n(t)\,\frac{df_n(T_m)}{dT_m}\,\dot{T}_m\right]$$

$$+ m_p c^2\left[\dot{N}_p(t)\, f_p(T_m) + N_p(t)\,\frac{df_p(T_m)}{dT_m}\,\dot{T}_m\right]$$

$$+ m_e c^2\left[\dot{N}_e(T_m,t)\, f_e(T_m) + N_e(T_m,t)\,\frac{df_e(T_m)}{dT_m}\,\dot{T}_m\right] . \qquad (3.49)$$

Using equations (3.4) and (3.26) and with $N_i = n_i V$ where V is the volume, the total number of neutrons N_n, total number of protons N_p, and total number of electrons plus positrons N_e, is respectively

$$N_n(t) = X_n(t)\, N_b \ , \qquad (3.50a)$$

$$N_p(t) = \left[1 - X_n(t)\right] N_b \ , \qquad (3.50b)$$

$$N_e(T_m,t) = N_{ep}(T_m) + N_{ed} + N_e^{decay}(t) \ , \qquad (3.50c)$$

where $N_e^{decay}(t) = N_{n0} - N_n(t) = N_{n0} - X_n(t)N_b$, is the total number of electrons released from the neutron decay at time t. The rate of change of N_n, N_p, and N_e is respectively

$$\dot{N}_n(t) = \dot{X}_n(t)\, N_b \ ,$$

$$\dot{N}_p(t) = -\dot{X}_n(t)\, N_b \ ,$$

$$\dot{N}_e(T_m,t) = \dot{N}_{ep}(T_m) - \dot{X}_n(t)\, N_b \ ,$$

where $\dot{X}_n(t) = - r_{np} X_n(t)$ (see equation (3.9)). Using equation (3.24) to evaluate $\dot{N}_{ep}$, the rate of change of N_e then becomes

$$\dot{N}_e(T_m,t) = \left[3\frac{\dot{R}}{R} + \left(\frac{3}{2T_m} + \frac{m_e c^2}{kT_m^2} \right) \dot{T}_m \right] N_{ep}(T_m) - \dot{X}_n(t)\, N_b \ . \tag{3.51}$$

Substituting (3.51) into the matter energy equation (3.49), and them substituting the new expression for $\dot{U}_m$ into the dynamical equation (3.45), we obtain

$$\begin{aligned} & m_n c^2 \left(\dot{N}_n(t)\, f_n(T_m) + N_n(t) \frac{df_n(T_m)}{dT_m} \dot{T}_m \right) \\ & + m_p c^2 \left(\dot{N}_p(t)\, f_p(T_m) + N_p(t) \frac{df_p(T_m)}{dT_m} \dot{T}_m \right) \\ & + m_e c^2 \left[\left(N_{ep}(T_m) \left[3\frac{\dot{R}}{R} + \left(\frac{3}{2T_m} + \frac{m_e c^2}{kT_m^2} \right) \dot{T}_m \right] - \dot{X}_n(t)\, N_b \right) f_e(T_m) \right. \\ & \left. + N_e(T_m,t) \frac{df_e(T_m)}{dT_m} \dot{T}_m \right] + 4\pi p_m(T_m) R^2 \dot{R} = \mathcal{E}_m(T_m,T_r) \end{aligned} \tag{3.52}$$

After rearrangment, equation (3.52) gives the rate of change of the matter temperature as

$$\dot{T}_m = \frac{1}{g_1(T_m,t)} \left[\mathcal{E}_m(T_m,T_r) - 4\pi p_m(T_m) R^2 \dot{R} - g_2(T_m,t) - 3m_e c^2 N_{ep}(T_m) f_e(T_m) \frac{\dot{R}}{R} \right] , \tag{3.53}$$

where the functions $g_1(T_m,t)$ and $g_2(T_m,t)$ are defined as

$$g_1(T_m,t) \equiv \left[N_{ep}(T_m)\, m_e c^2\, f_e(T_m) \left(\frac{3}{2T_m} + \frac{m_e c^2}{kT_m^2} \right) + \sum_{i=n,p,e} N_i(T_m,t)\, m_i c^2 \frac{df_i(T_m)}{dt} \right], \tag{3.54}$$

and

$$g_2(T_m,t) \equiv \sum_{i=n,p} \left(\dot{N}_i(t)\, m_i c^2\, f_i(T_m) \right) + \dot{X}_n(t)\, N_b\, f_e(T_m) . \tag{3.55}$$

Equation (3.53) is the dynamical equation for the matter written as a differential equation in T_m, and replaces the matter energy dynamical equation (3.45). The equations to solve are the four coupled differential equations (3.44), (3.46), (3.47), and (3.53), together with the neutron decay equation (3.10), and the interaction (3.43). A fourth order Runge-Kutta method (see for example Scheid 1968), is used to find a numerical solution (using a Fortran program) for the variables R, T_m, U_r, and U_ν as a function of time.

3.6 The later universe; oscillating model

The Thomson interaction (3.43) is very strong and is able to hold the matter and radiation temperatures together until the electrons and photons recombine at $T_m \simeq 4000$ K (Peebles 1971). After recombination the photons scatter off the resulting hydrogen atoms. Using a similar form to equation (3.43) but with the mass of a hydrogen atom, this interaction is found to have negligible effect. The neutrinos are noninteracting (except for gravitation) over the temperature range considered here and expand adiabatically with $T_{\nu_e}, T_{\nu_\mu} \propto R^{-1}$.

On contraction the matter temperature increases, the hydrogen is ionised and the interaction again becomes effective. The cycle was stopped, as in the continuum model, when the scale factor returned to its initial value. The final temperature was $2{\cdot}1 \times 10^9$ K, which is still below the temperature at which helium becomes unstable, i.e., 4×10^9 K at the final densities of $n_b \sim 10^{22}$ cm^{-3}, treated here (evaluated from equations (3.23) and (3.20))

Figure 4 shows the composition of the matter during the expanding phase. During the radiation-neutrino energy dominated era and after the e^-e^+ annihilation, one has $R \propto t^{1/2}$ because the radiation, like the neutrinos, expands essentially adiabatically (after the e^-e^+ have annihilated the energy transferred from the radiation to the remaining electrons by the Thomson interaction is very small relative to the total radiation energy U_r), with the radiation and neutrino energy densities ρ_r and ρ_ν, falling as R^{-4}. Also by equation (3.44) we have $\dot{R}^2 \propto (U_r + U_\nu)/R$ during this period, i.e., $\dot{R}^2 \propto R^{-2}$ or $R \propto t^{1/2}$. Hence the $\ln U_r$ and $\ln U_\nu$ curves in Figure 4 have slope $-\frac{1}{2}$ during the radiation-neutrino era.

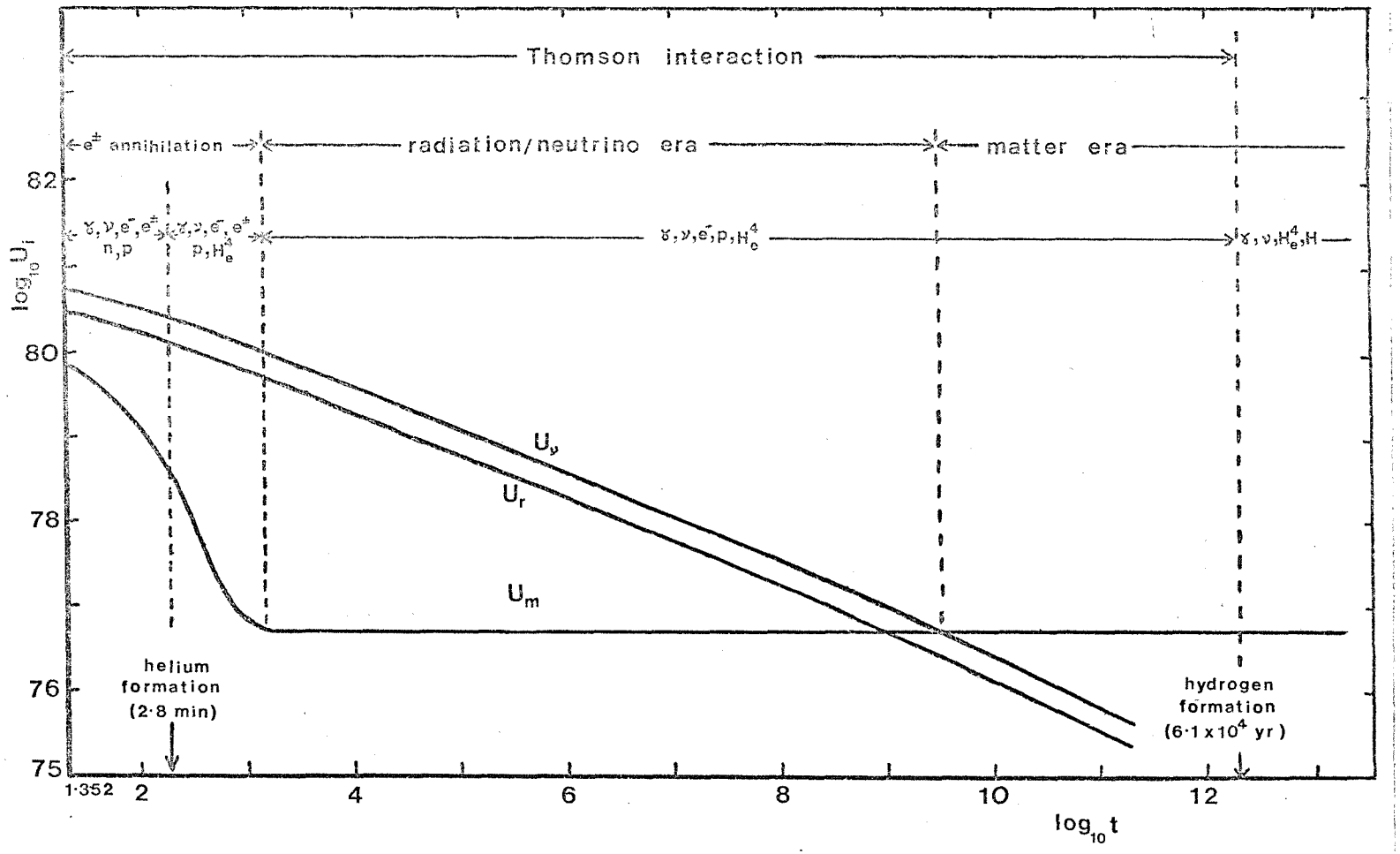

FIGURE 4 Model type : continuum-particle, Thomson interaction. The figure shows the total energy of the radiation U_r, the neutrinos U_ν, and the matter U_m, and the composition of the matter, on expansion.

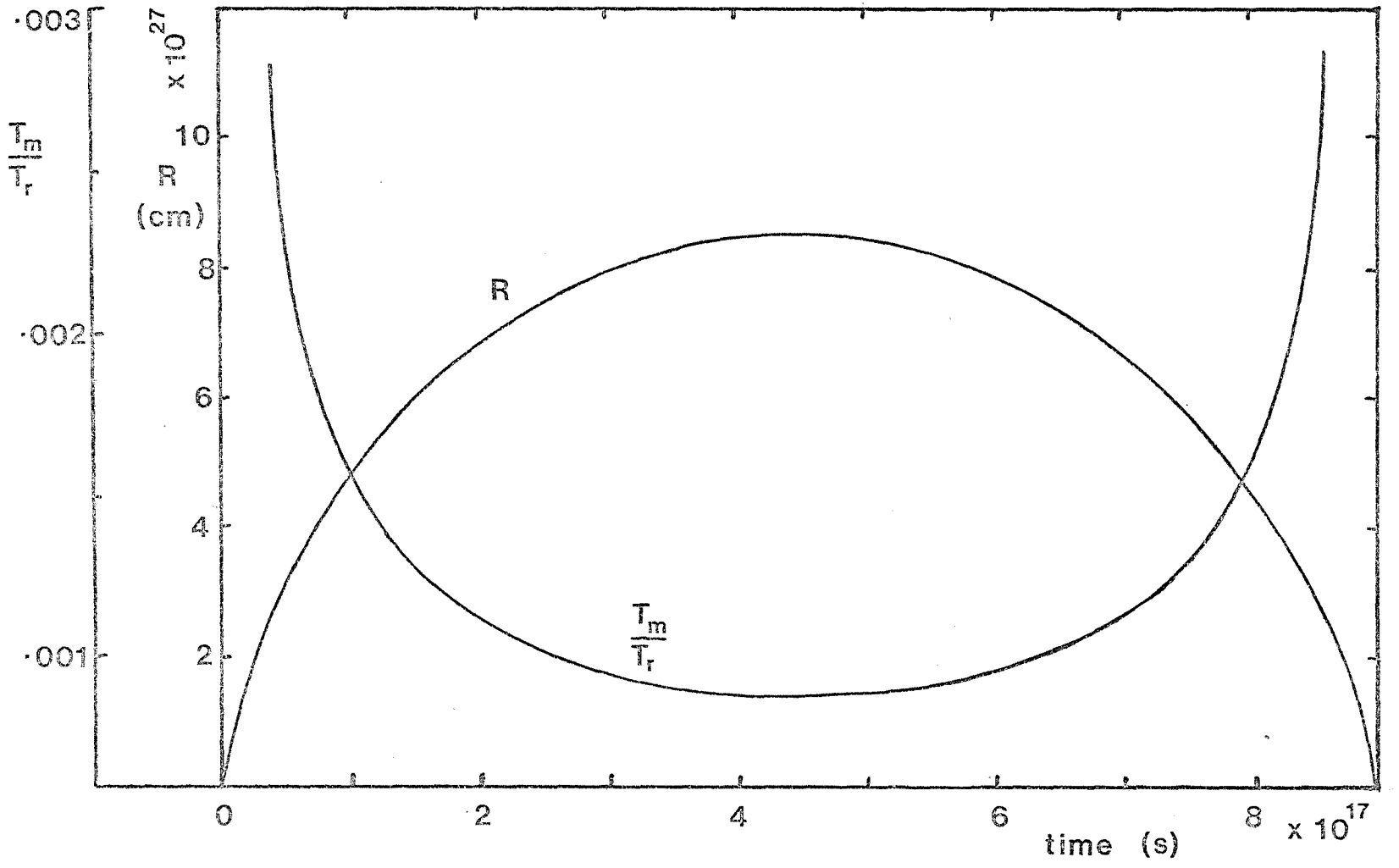

FIGURE 5 Model type : continuum-particle, oscillating, Thomson interaction. The figure illustrates the scale factor R and temperature ratio T_m / T_r for the computed cycle. The cycle time extends from $t = 22{\cdot}5$ s to $t = 9{\cdot}0 \times 10^{17}$ s.

After recombination when the model becomes matter dominated and when the curvature index term Kc^2 is still small relative to U_m/R, one has $R \propto t^{2/3}$ because the matter expands adiabatically with the matter energy density ρ_m falling as R^{-3}, and by equation (3.44) we have $\dot{R}^2 \propto U_m/R$, i.e., $\dot{R}^2 \propto R^{-1}$ or $R \propto t^{2/3}$. Hence the $\ln U_r$ and $\ln U_\nu$ curves in Figure 4 have slope $-2/3$ during this period. After the e^-e^+ annihilation the total matter energy U_m remains essentially constant at its rest mass value (Figure 4).

Figure 5 illustrates the scale factor R and temperature ratio T_m/T_r for the computed cycle. The cycle is almost, but not precisely, symmetrical about the time of maximum expansion.

Table II gives a comparison of the data between the initial and final states. As in the continuum model, they are not identical. The neutrino component in non-interacting and has identical initial and final energies, while the matter and radiation components have more energy in the final than in the initial state, with the radiation dominating this effect. The extra energy in the final state means an entropy increase of $3{\cdot}0 \times 10^{70}$ erg K^{-1}, i.e., an increase in the entropy per baryon of $6{\cdot}4 \times 10^6$ k during the cycle (S is defined to be zero initially).

3.7 The later universe; ever expanding model

The ever expanding continuum-particle model is of limited interest because the early stages are very similar to the oscillating model already discussed (Section 3.3), while the later stages develop like the ever expanding continuum model discussed in section 2.6. This model is therefore not pursued further.

Table II

Parameters for oscillating, Thomson interaction, continuum-particle model with $T_{m0} = T_{r0} = T_{\nu_e 0} = T_{\nu_\mu 0}$

Parameter	Initial state	Present state ($T_r = 2{\cdot}70$ K)	Maximum expansion	Final state
R (cm)	$8{\cdot}300 \times 10^{18}$	$6{\cdot}061 \times 10^{27}$	$8{\cdot}542 \times 10^{27}$	$8{\cdot}300 \times 10^{18}$
t (s)	22·24	$1{\cdot}561 \times 10^{17}$	$4{\cdot}495 \times 10^{17}$	$8{\cdot}990 \times 10^{17}$
U_m (erg)	$7{\cdot}022 \times 10^{79}$	$5{\cdot}170 \times 10^{76}$	$5{\cdot}170 \times 10^{76}$	$7{\cdot}104 \times 10^{79}$
ρ_b (g cm^{-3})	$2{\cdot}400 \times 10^{-2}$	$6{\cdot}163 \times 10^{-29}$	$2{\cdot}202 \times 10^{-29}$	$2{\cdot}400 \times 10^{-2}$
T_m (K)	$2{\cdot}000 \times 10^{9}$	$3{\cdot}366 \times 10^{-3}$	$1{\cdot}695 \times 10^{-3}$	$2{\cdot}096 \times 10^{9}$
U_r (erg)	$2{\cdot}900 \times 10^{80}$	$3{\cdot}749 \times 10^{71}$	$2{\cdot}660 \times 10^{71}$	$2{\cdot}952 \times 10^{80}$
T_r (K)	$2{\cdot}000 \times 10^{9}$	2·700	1·916	$2{\cdot}096 \times 10^{9}$
U_ν (erg)	$5{\cdot}073 \times 10^{80}$	$6{\cdot}948 \times 10^{71}$	$5{\cdot}926 \times 10^{71}$	$5{\cdot}073 \times 10^{80}$
$T_{\nu_e} = T_{\nu_\mu}$ (K)	$2{\cdot}000 \times 10^{9}$	2·739	1·943	$2{\cdot}000 \times 10^{9}$
U_{tot} (erg)	$8{\cdot}675 \times 10^{80}$	$5{\cdot}170 \times 10^{76}$	$5{\cdot}170 \times 10^{76}$	$8{\cdot}735 \times 10^{80}$
N_{ep}	$5{\cdot}327 \times 10^{85}$	0	0	$5{\cdot}442 \times 10^{85}$
H (Km s^{-1} Mpc^{-1})	$2{\cdot}816 \times 10^{17}$	97·66	0	$-2{\cdot}826 \times 10^{17}$
q	0·500	1·720	∞	0·500
S (erg K^{-1})	0	$1{\cdot}516 \times 10^{70}$	$1{\cdot}516 \times 10^{70}$	$3{\cdot}033 \times 10^{70}$
S/baryons	0	$3{\cdot}197 \times 10^{6}$ k	$3{\cdot}197 \times 10^{6}$ k	$6{\cdot}395 \times 10^{6}$ k

3.8 Discussion of the neutrino temperature

At the present epoch with $T_r = 2{\cdot}70$ K, the continuum-particle model predicted a nonstandard result, namely a neutrino temperature slightly above the radiation temperature at $T_{\nu_e} = T_{\nu_\mu}$ $(2{\cdot}74\ \mathrm{K}) > T_r\ (2{\cdot}70\ \mathrm{K})$. The standard calculation (eg., Peebles 1966; Wagoner, Fowler and Hoyle 1967) has $T_r(2{\cdot}70\ \mathrm{K}) > T_{\nu_e} = T_{\nu_\mu}$ $(1{\cdot}91\ \mathrm{K})$, and there are two physical reasons for this new result.

The first departure from the standard calculation arises because on the present model the neutrinos do not decouple at $\sim 5 \times 10^{10}$ K as assumed in the standard model, but at, or near, 2×10^9 K. The reason resides in the neutral and charge current reactions which help to couple the neutrinos with the matter via $e^{\pm} + \nu_e \rightarrow e^{\pm} + \nu_e$, $e^{\pm} + \bar{\nu}_e \rightarrow e^{\pm} + \bar{\nu}_e$, $e^+ + e^- \leftrightarrow \nu_e + \bar{\nu}_e$, and similar reactions for ν_μ (there may exist a third neutrino type ν_τ, but its inclusion in the model would not significantly change the results presented here). While the matter remains dominated by e^-e^+ pairs, i.e., down to around 2×10^9 K or so, these currents are able to lock the matter temperature to the neutrino temperature (Bludman 1976). This is the temperature at which the continuum-particle model is started, and it is thus reasonable to start with all components in equilibrium at that temperature. Thereafter the neutrinos are taken to be thermally noninteracting. The reasonableness of this argument is further supported by the observations of Weinberg (1974), who reports that the neutrinos go out of thermal equilibrium at temperatures somewhat above or below 3×10^9 K, and by Dolgov and Zeldovich (1981) who suggest that the neutrino and matter temperatures are locked down to $T < 0{\cdot}5$ MeV (i.e., $T < 3{\cdot}9 \times 10^9$ K if equipartition is used in the sense that kinetic energy is $3kT/2$).

Thus the energy and entropy released by the e^-e^+ annihilation after the temperature has fallen below

5×10^{10} K, was in the previous theories transferred solely to the radiation sea, but on the present initial conditions, the annihilation energy and entropy can be thought of as being fed also into the neutrino sea until the neutrinos decouple at $T \sim 2 \times 10^{9}$ K. The $e^{-}e^{+}$ pairs disappear at $\sim 5 \times 10^{8}$ K, and so their energy and entropy is transferred solely to the radiation sea only over the temperature range 2×10^{9} K to $\sim 5 \times 10^{8}$ K and not over the larger range 5×10^{10} K to $\sim 5 \times 10^{8}$ K as assumed in the standard model. The effect of this sharing of the annihilation energy between matter, radiation, and neutrinos above the temperature 2×10^{9} K, is thus to drag down T_m and T_r in the present model below what one would find in the standard work. T_{ν_e} and T_{ν_μ} are, relatively increased.

The second departure from the standard calculation depends on the fact that $m_e c^2/kT$ at 2×10^{9} K when the model starts, is already as large as 2·97. The pairs are therefore no longer extreme relativistic, although their kinetic energy is still significant because $3kT/2m_e c^2 \sim 0{\cdot}5$. The neutrinos are decoupled at this temperature, and if the matter and radiation are regarded as independent for the moment, then $T \propto R^{-s}$, where $1 < s \leqslant 2$ for matter and $s = 1$ for radiation and neutrinos. This means that energy is being transferred by the Thomson interaction from the radiation to the pairs, which is opposite to the direction of the energy transfer produced by $e^{-}e^{+}$ annihilation. Some of the kinetic energy of the pairs is continually being lost to the general expansion and hence further energy is transferred from the radiation to the pairs by the interaction to maintain equilibrium. The result of the interaction is therefore to lower T_r but not T_{ν_e} and T_{ν_μ} (as the neutrinos have decoupled). This effects terminates when the $e^{-}e^{+}$ have annihilated at $\sim 5 \times 10^{8}$ K. Figure 6 shows the ratio $(T_{\nu_e} - T_r)/T_r$ for the early universe (where $T_{\nu_e} = T_{\nu_\mu}$ at all times). After the annihilation period the ratio reaches a constant value since both T_{ν_e} and T_r fall like R^{-1}.

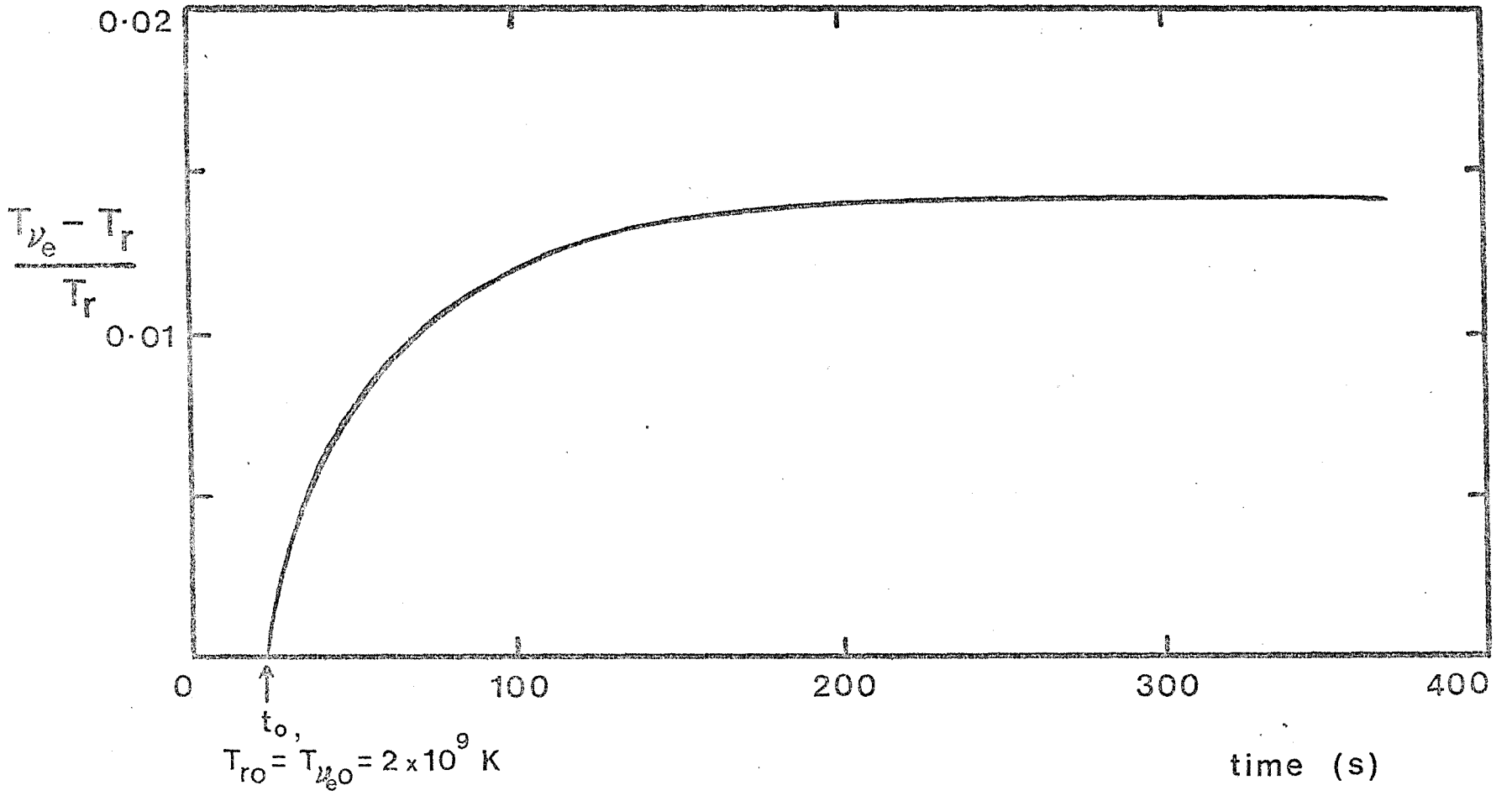

FIGURE 6 Model type : continuum-particle, Thomson interaction. The figure shows $(T_{\nu_e} - T_r)/T_r$ for the early universe. At time $t = 200$ s, 99·5% of the $e^- e^+$ have annihilated.

These arguments show that the value of the present day neutrino temperature is rather sensitive to the exact temperature at which the neutrino sea decouples from the other components. If the lepton neutrinos ν_e were to decouple at a different temperature to the muon neutrinos ν_μ then we would have today $T_{\nu_e} \neq T_{\nu_\mu}$. The result $T_{\nu_e} > T_r$ in the continuum-particle model implies that during the period when the temperature fell from 2×10^9 K to around 5×10^8 K, the energy transferred by the Thomson interaction from the radiation to the matter exceeded the energy gained by the radiation during this same period from the pair annihilation.

The models in this chapter began expansion at temperature 2×10^9 K with the matter semi-relativistic. The matter and radiation transferred energy according to the Thomson scattering formula (3.43). This interaction assumes however, that the velocity of the electrons is much less than the velocity of light, $v << c$, and that the radiation temperature is reasonably low $T_r < 10^7$ K. The models discussed here begin at temperatures greater than this, so one can ask is the Thomson scattering interaction a good approximation when $T_r > 10^7$ K and when $v \sim c$? Can a more general interaction be developed which takes into account the quantum and relativistic effects at high radiation temperatures and fast electron velocities, and how would this quantum-relativistic expression compare with the Thomson prediction as regards the matter-radiation energy transfer? These questions are addressed in the next chapter.

CHAPTER FOUR

THERMAL INTERACTION BETWEEN MATTER AND RADIATION IN THE EARLY UNIVERSE

THERMAL INTERACTION BETWEEN MATTER AND RADIATION IN THE EARLY UNIVERSE

4.1 Introduction

The models described in Chapters 2 and 3 made use of Thomson scattering between the photons and free electrons as the main matter-radiation thermal interaction. During expansion this interaction was easily capable of maintaining the matter and radiation in thermal equilibrium until the electrons and protons recombine, when the temperatures separate.

Strictly, Thomson scattering refers only to when the incident photon energy is much less than the rest energy of the electron. The change in the photon frequency due to the scattering is then negligible, and no energy is transferred between the electron and photon. More generally when the change in the photon frequency is important, is referred to as Compton scattering if the photon loses energy to the electron after scattering, and if the photon gains energy from the electron then it is often referred to as inverse Compton scattering. The interaction (3.43) gives the energy transferred between the matter and radiation by the Compton scattering when electron velocities are low and when radiation temperatures $T_r < 10^7$ K. However, in line with the literature (eg. Peebles 1971), we shall continue here to refer to the energy transfer equation (3.43) as the 'Thomson interaction'.

Thomson scattering has often been included in cosmological studies (see for example Felton and Morrison 1966; Peebles 1968; Pinkau 1980). If F_{Th} is the momentum transfer rate from blackbody radiation at temperature T_r to an electron moving with velocity v through the radiation, then

$$F_{Th} \propto -\frac{v}{c} T_r^4 , \qquad (4.1)$$

(Weyman 1965; Peebles 1971), where c is the velocity of light, and the negative sign indicates that the radiation acts as a drag force on the electron as it moves through the radiation. Equation (4.1) is derived by assuming the electron velocity is much less than the velocity of light $v \ll c$, and that the radiation temperature $T_r < 10^7$ K. Many cosmological studies begin at temperatures greater than this and it is the purpose of this chapter to show that at high radiation temperatures $T_r > 10^7$ K, and for electron velocities near the velocity of light $v \sim c$, the Thomson interaction must be generalised to take into account quantum and relativistic effects (Reeves and Landsberg 1982).

At high radiation temperatures $T_r > 10^7$ K, the scattering cross section of the electron is no longer a constant as given by the Thomson expression σ_{Th} (see equation (4.8) below), but becomes dependent on the incident radiation frequency. The Klein-Nishina cross section σ_{K-N} must then be used in full (σ_{Th} represents a special case). For the scattering of electrons and photons when $T_r > 10^7$ K, one needs to change to the more complicated σ_{K-N}, and for $v \sim c$ one must include the relativistic Doppler effect on the incident radiation frequency. This leads to the Klein-Nishina momentum transfer rate F_{K-N} (Section 4.2). For low radiation temperature and slow electron velocities it is shown that F_{K-N} becomes the classical expression F_{Th}, equation (4.1) (Section 4.3).

While it is known that at high radiation frequencies σ_{K-N} always lies below σ_{Th} (Heitler 1954; Tucker 1975), an explicit study of the resulting decrease of the theoretical momentum transfer rate for electron-photon scattering is discussed here for the first time. The dependence of F_{K-N} on T_r and v/c is illustrated graphically (Section 4.4), and in particular for $T_r \gg 1$ and $v/c \sim 1$, F_{K-N} is shown (equation (4.27) below) to have the dependence to first order in v/c;

$$F_{K-N} \propto -\frac{v}{c} T_r^3 \left[\ln(bT_r) + \frac{1}{2} \right], \qquad (4.2)$$

where b is a constant.

In the early universe when temperatures are high the helium and hydrogen atoms are ionised and the matter component comprises uniform distributions of nuclei and free electrons. This leads to the study of the momentum transfer rate from radiation to an equilibrium distribution of electrons and, using the Klein-Nishina formula, this transfer rate R_{K-N}, is worked out here for a range of electron temperatures T_e between 10^5 K and 10^{11} K, and for a range of blackbody radiation temperatures between 10^7 K and 10^{12} K (Section 4.5).

The transfer rate R_{K-N} is then discussed with the electrons and radiation in thermal equilibrium $T_e = T_r \equiv T$ ($T_e = T_r$ would apply to the early universe). It is shown (Section 4.5), that at temperatures $T \leqslant 10^7$ K the Klein-Nishina and Thomson expressions predict similar momentum transfer rates (although the net transfer rate is zero at $T_e = T_r$, the electrons and radiation will continue to exchange momentum at thermal equilibrium; the rate of momentum loss by the electrons as they move through the radiation will be equal and opposite to their momentum gain from the radiation due to the action of the Brownian motion of the photons). For electrons and radiation in thermal equilibrium at temperatures 10^7 K $< T < 5 \times 10^9$ K, the Klein-Nishina interaction predicted the transfer rate to lie below the corresponding Thomson transfer rate, i.e., the electrons and radiation are more weakly coupled at these temperatures in the Klein-Nishina case than in the classical Thomson case. However, at high temperatures $T > 5 \times 10^9$ K, the Klein-Nishina expression predicted the transfer rate to increase rapidly with increasing T and consequently to rise above the value predicted by the Thomson expression, i.e., the electrons and radiation are more strongly coupled at high temperatures with the Klein-Nishina interaction than with the corresponding Thomson interaction.

4.2 The Klein-Nishina interaction

We take blackbody radiation which is isotropic in a frame E_0 and an electron moving with a velocity v along the X-direction in E_0. The radiation intensity (energy per unit area per second) in a frequency interval $\nu_0 \rightarrow \nu_0 + d\nu_0$ and solid angle interval $\Omega_0 \rightarrow \Omega_0 + d\Omega_0$, in the frame E_0 is given by the Planck spectrum as (see for example Pauli 1958),

$$I_0(\nu_0)\, d\nu_0\, d\Omega_0 = \frac{2h}{c^2} \frac{\nu_0^3}{\left[\exp\left(\frac{h\nu_0}{kT_{r0}}\right) - 1\right]} d\nu_0\, d\Omega_0 , \quad (4.3)$$

where T_{r0} is the isotropic radiation temperature.

If I and ν are the radiation intensity and radiation frequency as measured in the rest frame of the electron E, and using the invariance property $I_0/\nu_0^3 = I/\nu^3$ between the two frames E_0 and E, then the radiation intensity in a frequency interval $\nu \rightarrow \nu + d\nu$ and solid angle interval $\Omega \rightarrow \Omega + d\Omega$ in the electron's frame E becomes

$$I\, d\nu\, d\Omega = \frac{I_0}{\nu_0^3} \nu^3\, d\nu\, d\Omega$$

$$= \frac{2h}{c^2} \frac{\nu^3}{\left[\exp\left(\frac{h\nu_0}{kT_{r0}}\right) - 1\right]} d\nu\, d\Omega . \quad (4.4)$$

Expressing ν_0 in the exponent of equation (4.4) as a

function of the electron system frequency ν, and if θ is the angle between the X-axis and the direction of the incident photon as measured in the electron's frame E, then the transformation for ν_0 is (see eg., Jackson 1962, eqn. (11.38)),

$$\nu_0 = \nu \frac{1 + \beta \cos\theta}{(1 - \beta^2)^{\frac{1}{2}}} \quad , \tag{4.5}$$

where $\beta \equiv v/c$. The radiation intensity equation (4.4) is then

$$I(\nu,\nu,\theta)\, d\nu\, d\Omega = \frac{2h}{c^2} \frac{\nu^3\, d\nu\, d\Omega}{\left[\exp\left(\frac{h\nu}{kT_{r0}} \cdot \frac{1+\beta\cos\theta}{(1-\beta^2)^{\frac{1}{2}}}\right) - 1\right]} . \tag{4.6}$$

The electron cross section σ_{K-N}, in E is given by the Klein-Nishina scattering cross section (Pomraning 1973),

$$\sigma_{K-N}(\nu) = \frac{3}{4}\sigma_{Th}\left[\frac{1 + z(\nu)}{z^3(\nu)}\left(\frac{2z(\nu)[1 + z(\nu)]}{1 + 2z(\nu)} - \ln[1 + 2z(\nu)]\right)\right.$$

$$\left. + \frac{1}{2z(\nu)} \ln[1 + 2z(\nu)] - \frac{1 + 3z(\nu)}{[1 + 2z(\nu)]^2}\right] . \tag{4.7}$$

Here $z(\nu) \equiv h\nu/(m_e c^2)$, ν is the incident radiation frequency as measured in frame E, and m_e is the rest mass of the electron. The Thomson scattering cross

section is (Heitler 1954),

$$\sigma_{Th} = \frac{8}{3}\pi\left(\frac{e^2}{m_e c^2}\right)^2 = 6{\cdot}65 \times 10^{-25} \text{ cm}^2 , \qquad (4.8)$$

where e is the electronic charge.

At low radiation frequencies $z \ll 1$, and using the expansion $\ln(1+x) = x - \frac{1}{2}x^2 + \frac{1}{3}x^3 - \frac{1}{4}x^4 + \ldots$, the cross section σ_{K-N} simplifies to

$$\sigma_{K-N} = \frac{3}{4}\sigma_{Th}\left[\frac{1+z}{z^3}\left(2z\,(1 - z + 2z^2 - 4z^3 + 8z^4 + \ldots)\right.\right.$$

$$\left. - \left(2z - 2z^2 + \frac{8}{3}z^3 - 4z^4 + \frac{32}{5}z^5 + \ldots\right)\right) + (1 - z$$

$$\left. + \frac{4}{3}z^2 - 2z^3 + \ldots) - (1 - z + 4z^3 + \ldots)\right]$$

$$= \frac{3}{4}\sigma_{Th}\left[(1+z)\left(\frac{4}{3} - 4z + \frac{48}{5}z^2 - \ldots\right) + \frac{4}{3}z^2 + \ldots\right]$$

$$= \sigma_{Th}\left(1 - 2z + \frac{26}{5}z^2 + \ldots\right), \quad m_e c^2 \gg h\nu . \qquad (4.9)$$

At high radiation frequencies $z \gg 1$, and using the approximation $(1+z) \simeq z$, σ_{K-N} becomes,

$$\sigma_{K-N} \simeq \frac{3}{4}\sigma_{Th}\left[\frac{1}{z^2}\left[z - \ln(2z)\right] + \frac{1}{2z}\ln(2z) - \frac{3}{4z}\right]$$

$$\simeq \frac{3}{8}\sigma_{Th}\,\frac{1}{z}\left[\ln(2z) + \frac{1}{2}\right], \quad m_e c^2 \ll h\nu . \qquad (4.10)$$

There will be a momentum transfer to the electron along the X-direction due to the action of the radiation (the radiation acts as a drag force). The momentum intensity of the radiation (momentum per unit area per second) in a frequency interval $\nu \to \nu + d\nu$ and solid angle interval $\Omega \to \Omega + d\Omega$, as measured in the electron frame E will be $I(\nu,\nu,\theta)\, d\nu\, d\Omega / c$. The rate of momentum transfer to the electron in this frequency and solid angle interval will then be

$$\sigma_{K-N}(\nu)\ \frac{I(\nu,\nu,\theta)\, d\nu\, d\Omega}{c}\ \cos\theta\ . \qquad (4.11)$$

Integrating over all frequencies and solid angles gives the total rate of momentum transfer to the electron:

$$F_{K-N}(\nu) \equiv \frac{dp_{K-N}(\nu)}{dt}$$

$$= \int_{\nu}\int_{\Omega} \sigma_{K-N}(\nu)\ \frac{I(\nu,\nu,\theta)}{c}\ \cos\theta\ d\nu\, d\Omega\ . \qquad (4.12)$$

For an equilibrium distribution of electrons of total number N_e interacting with the radiation, the rate of momentum transfer R_{K-N}, will be

$$R_{K-N} = \int_{\nu} F_{K-N}(\nu)\, N_e\, s(\nu)\, d\nu\ , \qquad (4.13)$$

where $s(\nu)\, d\nu$ is the probability that the speed of an electron lies between ν and $\nu + d\nu$. In the standard model of the early universe, the electron temperature T_e

is sufficiently high, and the electron number density n_e sufficiently low for the nondegeneracy condition; $n_e h^3 (\pi k m_e)^{-3/2} \ll 1$, to be easily satisfied, and hence for the electrons to have vanishingly small chemical potential (Weinberg 1972). It is then possible to write as a relativistic Maxwell-Boltzmann distribution (Wienke 1975),

$$s(v) = m_{e*}^3 \, \delta^{-1} \, \frac{v^2}{(1-\beta^2)} \, \exp\left(\frac{E(v)}{kT_e}\right) , \qquad (4.14)$$

where m_{e*} is the relativistic electron mass and $E(v) = m_{e*} c^2 = m_e c^2/(1-\beta^2)^{\frac{1}{2}}$ is the total relativistic energy of the electron. The constant δ has the value

$$\delta = m_e^2 \, ckT_e \, K_2(m_e c^2/kT_e) , \qquad (4.15)$$

and ensures that the distribution (4.14) is correctly normalised with $\int_v s(v)\, dv = 1$. $K_2(y)$ is the modified Bessel function of second order,

$$K_2(y) = \frac{\Gamma(\frac{1}{2})\,(y/2)^2}{\Gamma(\frac{5}{2})} \int_1^\infty e^{-yt} \, (t^2-1)^{\frac{3}{2}} \, dt ,$$

and $\Gamma(n)$ is the gamma function,

$$\Gamma(n) = \int_0^\infty x^{n-1} \, e^{-x} \, dx , \quad n > 0 .$$

4.3 The classical limit ; the Thomson interaction

For any constant cross section such as equation (4.8), one has

$$F_{Th}(\nu) \equiv \frac{dp_{Th}(\nu)}{dt}$$

$$= \sigma_{Th} \int_{\nu} \int_{\Omega} \frac{2h}{c^3} \frac{\nu^3 \cos\theta \; d\nu \; d\Omega}{\left[\exp\left(\frac{h\nu}{kT_{r0}} \cdot \frac{1 + \beta\cos\theta}{(1-\beta^2)^{\frac{1}{2}}} \right) - 1 \right]} \cdot \quad (4.16)$$

To integrate equation (4.16) over frequency ν, the following two relations prove useful,

$$\frac{x^3}{e^{bx} - 1} = \sum_{n=0}^{\infty} x^3 \, e^{-b(n+1)x} \quad , \quad (4.17)$$

where $e^{-bx} < 1$, and (see eg., Abramowitz and Stegun 1972, p255),

$$\int_0^{\infty} e^{-y} \, y^n \, dy = n! \quad (4.18)$$

Writing $x \equiv h\nu/kT_{r0}$ and $b \equiv (1 + \beta\cos\theta)/(1 - \beta^2)^{\frac{1}{2}}$, and using the relation (4.17) in equation (4.16), we obtain

$$F_{Th}(\nu) = \sigma_{Th} \int_{\Omega} \cos\theta \; d\Omega \int_{x} 2 \frac{[kT_{r0}]^4}{(ch)^3} \sum_{n=0}^{\infty} x^3 \, e^{-b(n+1)x} \, dx \quad , \quad (4.19)$$

where x ranges from $0 \rightarrow \infty$. Now writing $y \equiv -b(n+1)x$ and $x^3 = -y^3/(b^3(n+1)^3)$, and with the result (4.18), equation (4.19) becomes

$$F_{Th}(\nu) = \sigma_{Th} \int_{\Omega} \cos\theta \, d\Omega \, 2 \frac{[kT_{r0}]^4}{(ch)^3} \sum_{n=0}^{\infty} \frac{3!}{b^4(n+1)^4} . \quad (4.20)$$

The summation term in equation (4.20) can be evaluated by using the standard result (Abramowitz and Stegun 1972, p807),

$$\sum_{m=0}^{\infty} \frac{1}{(m+1)^4} = \sum_{m=1}^{\infty} \frac{1}{m^4} = \frac{\pi^4}{90} . \quad (4.21)$$

Substituting (4.21) into equation(4.20) and writing $a = 8\pi^5 k^4/(15c^3h^3) = 7{\cdot}5641 \times 10^{-15}$ erg cm^{-3} K^{-4} , one has

$$F_{Th}(\nu) = \sigma_{Th} \frac{2}{15} \frac{(\pi k)^4}{(ch)^3} T_{r0}^4 \int_{\Omega} \frac{\cos\theta}{b^4} \, d\Omega$$

$$= \sigma_{Th} \frac{aT_{r0}^4}{2} \int_0^{\pi} \frac{(1-\beta^2)^2}{(1+\beta\cos\theta)^4} \cos\theta \sin\theta \, d\theta , \quad (4.22)$$

where a is the blackbody constant. Neglecting β^2 terms and higher and integrating over θ , F_{Th} finally becomes,

$$F_{Th}(v) = \sigma_{Th} \frac{aT_{r0}^4}{2} \int_0^{\pi} (\cos\theta - 4\beta\cos^2\theta + \ldots) \sin\theta \, d\theta ,$$

and after integration over θ, yields

$$F_{Th}(v) = -\frac{4}{3} \sigma_{Th} \, aT_{r0}^4 \, \frac{v}{c} . \qquad (4.23)$$

The negative sign in equation (4.23) indicates, as expected, that the force is in the direction opposite to the electron's motion. For an equilibrium distribution of electrons interacting with the radiation, the transfer rate with Thomson scattering R_{Th}, will be

$$R_{Th} = \int_v F_{Th}(v) \, N_e \, s(v) \, dv . \qquad (4.24)$$

Multiplying F_{Th}, equation (4.23), by the electron velocity v, will give the rate of change of the electron's energy, ε say, and defining the electron temperature T_e by the equipartition law $\frac{3}{2}kT_e = \frac{1}{2}m_e v^2$, we have for ε,

$$\varepsilon = v F_{Th} = -\frac{4\sigma_{Th} \, akT_{r0}^4}{m_e c} T_e .$$

Imposing the constraint that when $T_{r0} = T_e$ the rate of energy loss by the electron will be equal to its rate of energy gain from the radiation, we can expect the <u>net</u> rate of energy transfer to the electron, ε_e say, when $T_{r0} \neq T_e$

to be,

$$\varepsilon_e = \frac{4\sigma_{Th}\, akT_{r0}^4}{m_e c}(T_{r0} - T_e) , \qquad (4.25)$$

which satisfies the condition $\varepsilon_e = 0$ when $T_{r0} = T_e$. Equation (4.25) is the interaction per electron used in the continuum-particle model (see equation (3.43)).

4.4 Single electron moving through blackbody radiation

The Klein-Nishina expression for the single electron case, equation (4.12), was integrated numerically and a comparison was made with the corresponding Thomson case, equation (4.23) (Figure 7). The numerical procedure adopted to evaluate the integrals in (4.12) was taken from the University of Southampton 'NAG' computer library, routine D01 DAF developed from Patterson 1968.

Figure 7 shows the ratio F_{K-N}/F_{Th} over a radiation temperature range up to 10^{12} K and for two values of the electron velocity, 10 cm s^{-1} and $0{\cdot}9c$. The ratio decreases with increasing temperature. This means that the radiation temperature dependence of the momentum transfer rate, F, from the radiation to the electron is weaker when the Klein-Nishina formula is used than the T^4-law given by equation (4.23). Although it is known that at high radiation temperatures σ_{K-N} always lies below σ_{Th}, the decrease in the dependence of the transfer rate F_{K-N} on the radiation temperature has not been shown in detail before.

In regard to the dependence on the electron velocity v for a given radiation temperature, one has $F \propto v$ in the Thomson case and a stronger than linear

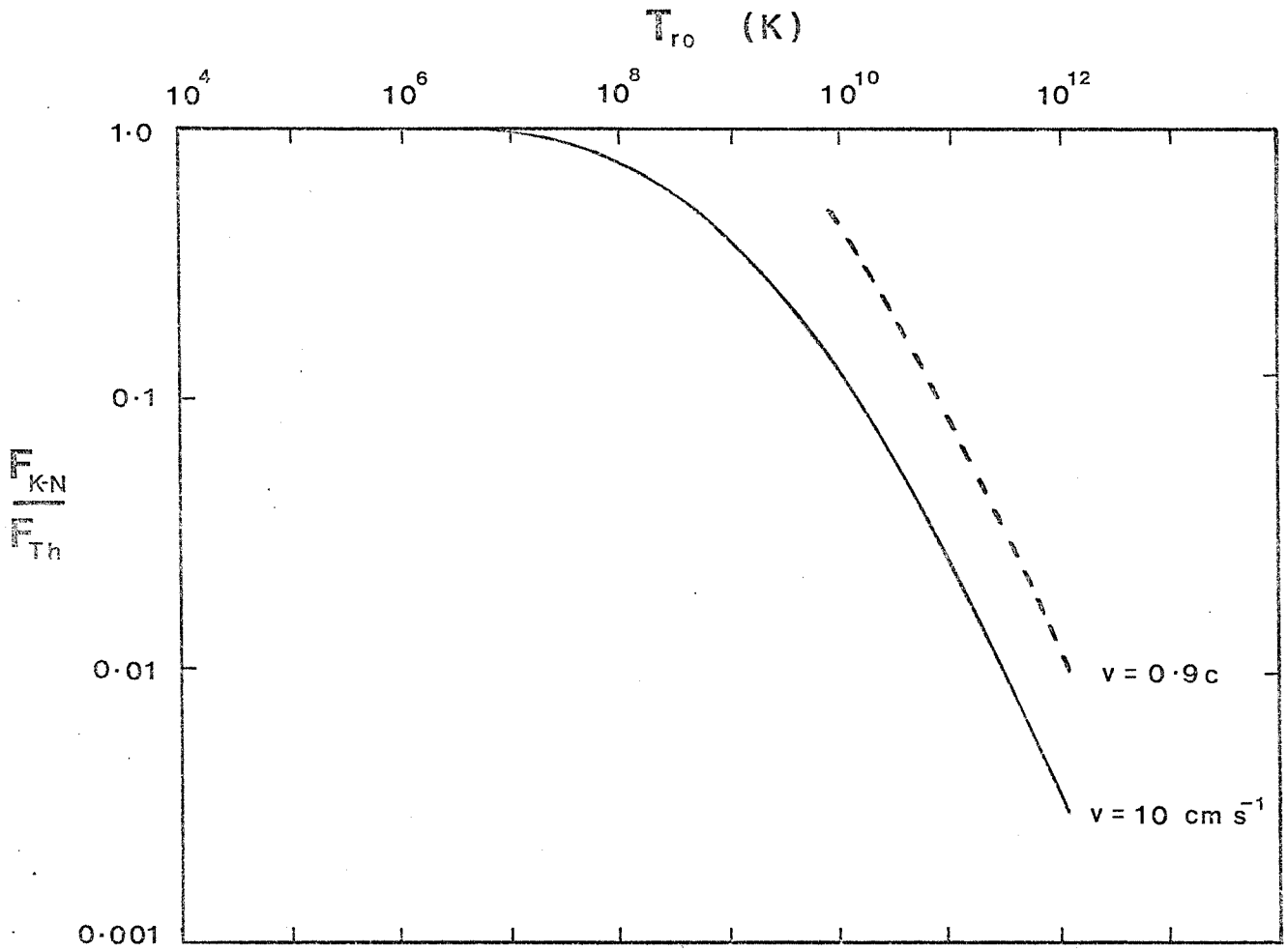

FIGURE 7 Single electron moving through blackbody radiation. The figure shows the ratio of the momentum transfer rates for the Klein-Nishina to Thomson interaction F_{K-N}/F_{Th}. Solid curve, v = 10 cm s^{-1} ; dashed curve, v = 0·9c .

dependence at the higher temperatures (where the Klein-Nishina formula must be used). This gives the effect of having the high velocity curve lying above the curve for nonrelativistic velocities in the figure. The velocity dependence is due to the radiation intensity, equation (4.6). In the Thomson case (where F is conventionally derived by going to first order in v/c only, as in equation (4.23)), σ_{Th} is a constant, whereas in the Klein-Nishina case the cross section σ_{Th}, equation (4.7), is frequency dependent. Although electron-positron and other particle-antiparticle pairs form at radiation temperatures $\sim 10^9$ K and higher, the matter and radiation are always close to thermal equilibrium and hence the blackbody distribution, equation (4.6), is still valid.

Figure 7 shows that for fixed T_{r0} the ratio F_{K-N}/F_{Th} increases when the electron velocity is increased from 10 cm s^{-1} to 0·9c. This result can be checked analytically by discussing the velocity dependence of F_{K-N} in the limiting case of $T_{r0} \gg 1$ and $v \sim c$. The scattering cross section is then given by equation (4.10), and to a good approximation the blackbody radiation distribution at high temperatures can be described by one major frequency, $\nu_{max} = cT_{r0}/(0{\cdot}289 \text{ cm K})$. The cross section (4.10) then becomes

$$\sigma_{K-N}(T_{r0}) = \frac{3}{4} \frac{\sigma_{Th}}{bT_{r0}} \left[\ln(bT_{r0}) + \frac{1}{2} \right] , \qquad (4.26)$$

where $b = 2h/(0{\cdot}289\, m_e c)$ cm^{-1} K^{-1}. Substituting the cross section (4.26) and the radiation intensity equation (4.6), into the momentum transfer rate F_{K-N}, equation (4.12), and again using the relations (4.17) and (4.18) to evaluate a similar integral over frequency ν as treated in equations (4.16) to (4.22), one obtains

$$F_{K-N} = \int_{\nu}\int_{\Omega} \frac{3}{4}\frac{\sigma_{Th}}{bT_{r0}}\left[\ln(bT_{r0}) + \frac{1}{2}\right] \frac{2hc^{-3}\,\nu^3 \cos\theta \; d\nu \, d\Omega}{\left[\exp\left(\frac{h\nu}{kT_{r0}} \cdot \frac{1+\beta\cos\theta}{(1-\beta^2)^{\frac{1}{2}}}\right) - 1\right]}$$

$$= \frac{3}{4}\sigma_{Th}\frac{aT_{r0}^4}{2bT_{r0}}\left[\ln(bT_{r0}) + \frac{1}{2}\right]\int_0^{\pi} \frac{(1-\beta^2)^2}{(1+\beta\cos\theta)^4}\cos\theta\,\sin\theta\,d\theta$$

Neglecting β^6 terms and higher and then integrating over θ, one has

$$F_{K-N} = \frac{3}{8}\sigma_{Th}\frac{aT_{r0}^3}{b}\left[\ln(bT_{r0}) + \frac{1}{2}\right](1 - 2\beta^2 + \beta^4)\int_0^{\pi}\frac{\cos\theta\,\sin\theta\,d\theta}{(1+\beta\cos\theta)^4}$$

$$= \frac{3}{8}\sigma_{Th}\frac{aT_{r0}^3}{b}\left[\ln(bT_{r0}) + \frac{1}{2}\right](1 - 2\beta^2 + \beta^4)\left(-\frac{8}{3}\beta - 8\beta^3 - 16\beta^5 - \ldots\right)$$

$$= -\sigma_{Th}\frac{aT_{r0}^3}{b}\left[\ln(bT_{r0}) + \frac{1}{2}\right]\beta(1 + \beta^2 + \beta^4 + \ldots), \qquad (4.27)$$

where $T_{r0} \gg 1$ and $v \sim c$. The negative sign in (4.27) indicates that the force is in the direction opposite to the electron's motion. Dividing (4.27) by the Thomson transfer F_{Th}, equation (4.23), the ratio of the Klein-Nishina to Thomson transfer rate leads to

$$\frac{F_{K-N}}{F_{Th}} = \frac{3}{4}\frac{1}{bT_{r0}}\left[\ln(bT_{r0}) + \frac{1}{2}\right](1 + \beta^2 + \beta^4 + \ldots).$$

Thus, as the electron becomes relativistic, β increases and brings the ratio F_{K-N}/F_{Th} closer to 1, as confirmed in Figure 7.

4.5 Equilibrium distribution of electrons interacting with blackbody radiation

For an equilibrium distribution of electrons immersed in a sea of blackbody radiation, Figure 8 shows the momentum transfer rate per electron R_{K-N}/N_e, (based on equations (4.13) and (4.12)), for a range of electron temperatures T_e, against radiation temperature T_{r0} (the triple integral arising from equations (4.13) and (4.12) was evaluated by Routine D01 FCF,'NAG' Computer Library, developed from Dooren and Ridder 1976). R_{K-N} is negative because the radiation acts as a drag force on the moving electrons, and this drag increases (becomes more negative) with increasing T_e and T_{r0}. In particular, for constant T_e, the drag increases slighty less rapidly with each increase in T_{r0} (the curves in Figure 8 have slighty decreasing slopes), whereas for constant T_{r0} the drag increases rapidly with each increase in T_e because the radiation intensity, equation (4.6), rises rapidly in the electron's direction of motion as $v \rightarrow c$.

R_{K-N} represents the rate of change of the momentum of the electrons as they travel through the radiation sea. The electrons will not come to rest because they will also gain momentum from the action of the Brownian motion of the radiation. The net rate of momentum transfer will be given by the difference between these two mechanisms, and in particular, when $T_e = T_{r0}$ the net transfer must fall to zero, i.e., the rate of momentum gain will be equal and opposite to R_{K-N} (equation (4.13))

Although the net transfer between the electrons and radiation is zero when $T_e = T_{r0}$, the electron and radiation will continue to exchange energy and momentum during thermal equilibrium. The magnitude of the total momentum transfer rate at thermal equilibrium will be twice $|R_{K-N}|$ because the electrons will gain momentum from the action of the Brownian motion of the photons at the same rate as they lose momentum through the radiation drag.

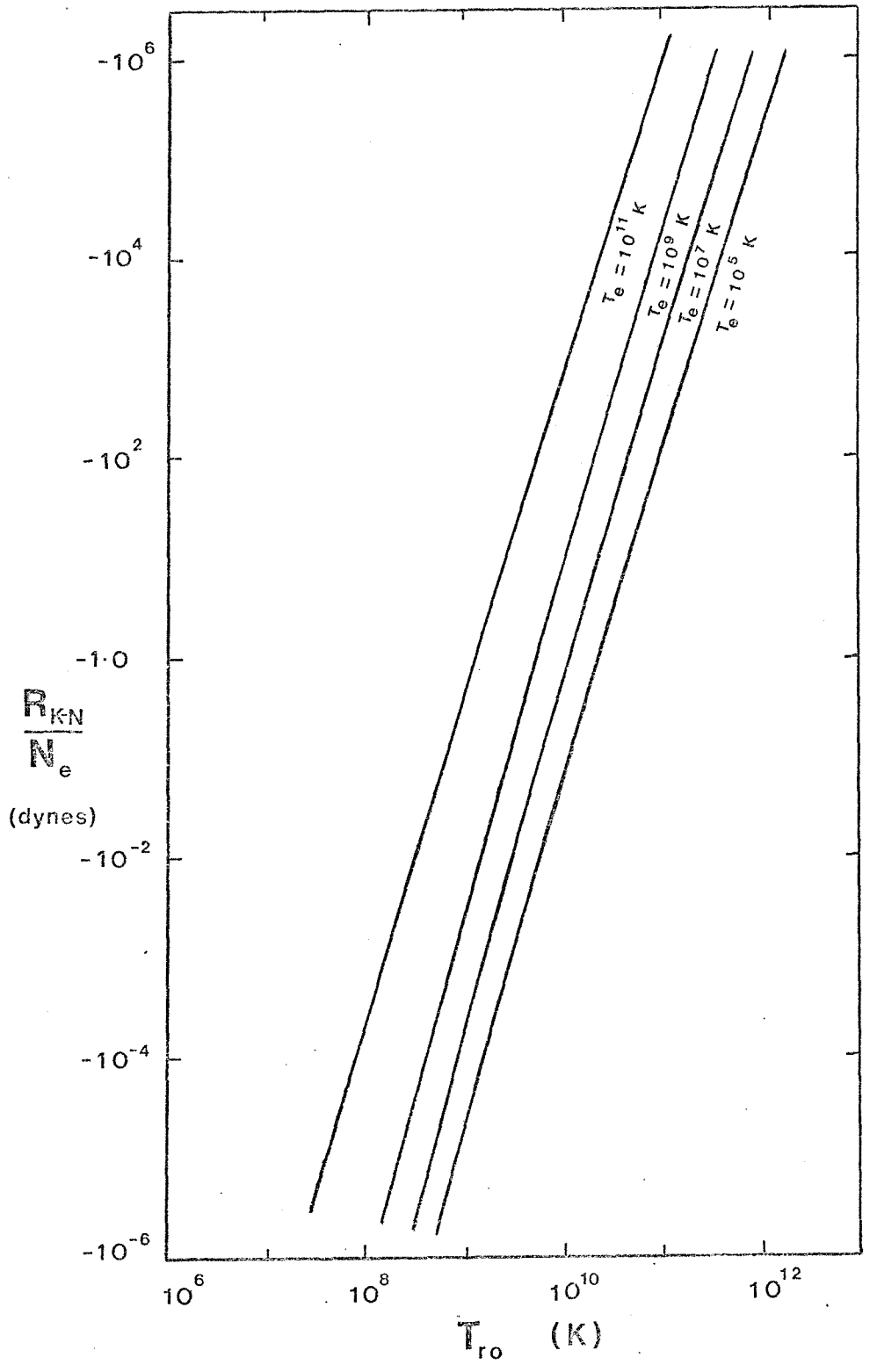

FIGURE 8 Equilibrium distribution of electrons interacting with blackbody radiation. The figure illustrates the momentum transfer rate per electron R_{K-N}/N_e against T_{rO} for a range of electron temperatures T_e.

Figure 9 makes a comparison between the momentum transfer rate at thermal equilibrium, $T \equiv T_e = T_{r0}$, for the Klein-Nishina and Thomson cases by illustrating R_{K-N}/R_{Th} for a range of temperatures T between 10^6 K and 10^{12} K. The figure shows that for electrons and radiation in equilibriun at temperatures $T < 10^7$ K, then $R_{K-N}/R_{Th} \sim 1$, i.e., the Thomson expression R_{Th} is in good agreement with the Klein-Nishina formula R_{K-N} at temperatures below 10^7 K. A temperatures $10^7 \text{ K} < T < 5 \times 10^9$ K the Klein-Nishina formula predicted a lower momentum transfer rate than that predicted by the Thomson case, i.e., the Klein-Nishina interaction has the electrons and radiation more <u>weakly</u> coupled in this temperature range than the corresponding Thomson interaction prediction. However, at higher temperatures $T > 5 \times 10^9$ K, Figure 9 shows that the Klein-Nishina expression predicted the momentum transfer rate to increase rapidly with increasing T and consequently to rise above the value predicted by the Thomson formula, i.e., the electrons and radiation are more <u>strongly</u> coupled at high temperatures in the Klein-Nishina interaction case than in the corresponding Thomson scattering case. The strong coupling at high temperatures $T > 5 \times 10^9$ K predicted by the Klein-Nishina interaction results from the incident radiation intensity increasing rapidly in the direction opposite to the electron's motion as $v \rightarrow c$ owing to the relativistic Doppler effect.

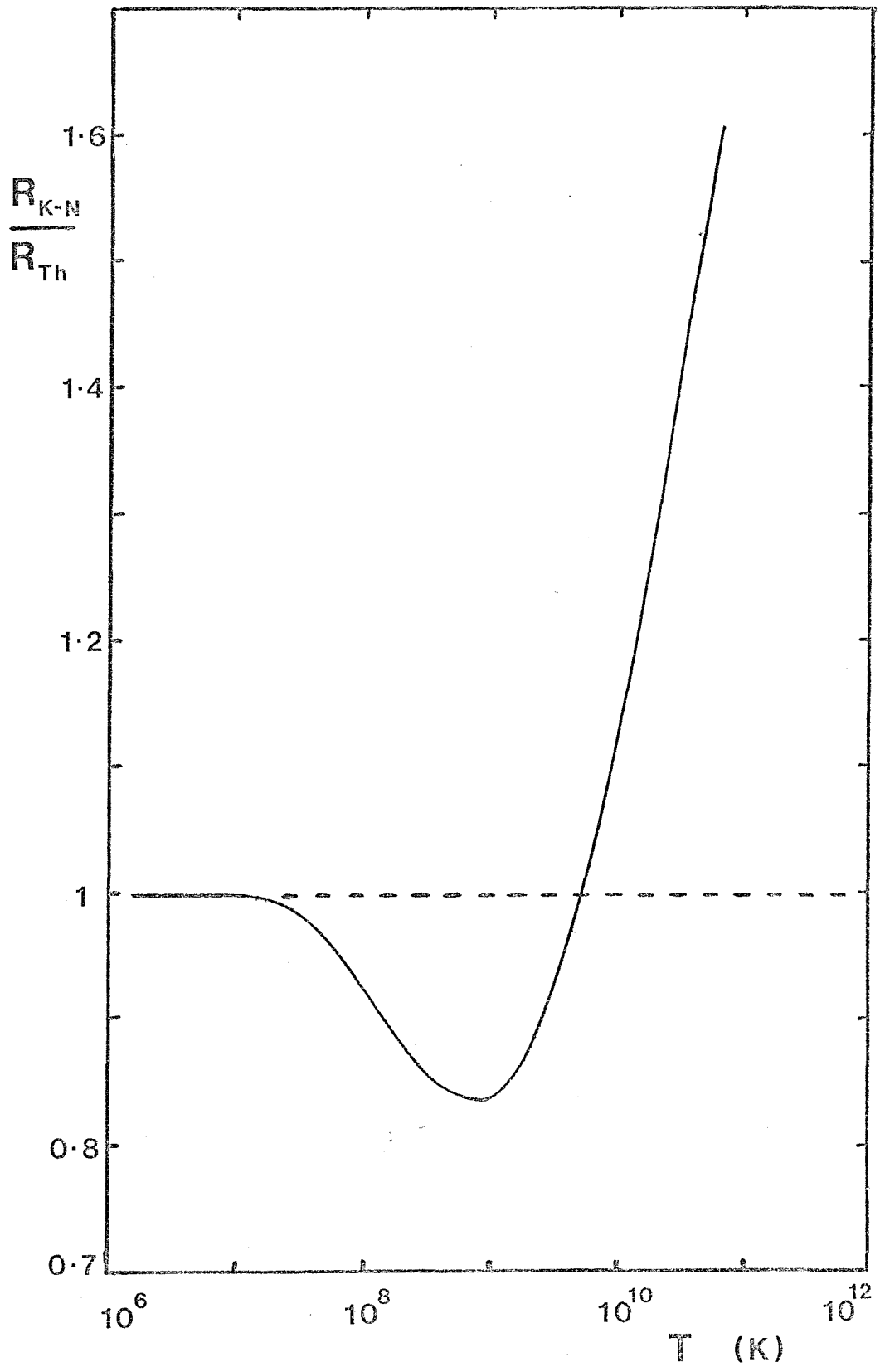

FIGURE 9 Equilibrium distribution of electrons interacting with radiation. The figure shows the ratio of the momentum transfer rate for the Klein-Nishina to Thomson interaction R_{K-N}/R_{Th}, for electrons and radiation in thermal equilibrium $T_e = T_{r0} \equiv T$

CHAPTER FIVE

CONCLUSION

CONCLUSION

The general thermodynamics of model universes have been studied by means of continuum and continuum-particle models. The former have been considered in earlier literature and this investigation begins with a further development of such models (Chapter 2). A continuum-particle theory is then devised. This model is a generalisation of the continuum theory and is introduced here for the first time (Chapter 3). Universes with oscillation and indefinite expansion have been discussed for both model types. Cutting out the singularities, the follow points have been found ;

(1) A new feature of ever expanding models is pointed out, namely that there is a maximum in the temperature difference $T_r - T_m$, before the 'heat death' is approached (Figure 2). This is accompanied by a drop in the matter-radiation interaction to such an extent that the matter and radiation develop independently and each component expands adiabatically and with constant entropy (Figure 3).

(2) A radiative T^4- and a Thomson scattering interaction between matter and radiation have been investigated for continuum models. It is found that (a) the general performance of ever expanding and oscillating models is rather insensitive to the choice between them; and (b) the entropy generated depends quite strongly on the interaction (Figure 3). Confirming earlier work, it is also found that the entropy increases even in the contracting phase (Figure 1).

(3) On terminating the contraction of an oscillating model at the initial scale factor, one finds for the final values relative to the initial values in both continuum and continuum-particle models (Tables IA and II) :
(a) The numerical value of the rate of change of the scale

factor is increased ; (b) The energy densities and entropies of both matter and radiation are increased.

(4) Considering a continuum-particle, oscillating, Thomson scattering model the following points emerge :
(a) Starting at $2{\cdot}0 \times 10^9$ K, approximately 22 seconds after the 'big bang', and terminating at the appropriate scale factor, it is found that the matter and radiation temperatures have increased slighty to $2{\cdot}1 \times 10^9$ K, while the neutrino component, which is thermally noninteracting, has identical initial and final temperatures (Table II). The cycle is almost, but not precisely, symmetric about the instant of maximum expansion (Figure 5).
(b) At the present epoch with $T_r = 2{\cdot}70$ K, the neutrino temperature is predicted to be slighty above this value at $T_{\nu_e} = T_{\nu_\mu} = 2{\cdot}74$ K (Figure 6). This is due to (i) the neutral and charge current reactions which encourage the neutrinos to stay in thermal equilibrium with the matter to around 2×10^9 K ; and (ii) the Thomson interaction which produces a reasonably large transfer of energy from the radiation to the matter before the disappearance of the e^-e^+ pairs at around 5×10^8 K (Figure 4).
(c) The extra energy in the final state when compared to the initial state means an increase of $3{\cdot}0 \times 10^{70}$ erg K^{-1} in the entropy of the model. This corresponds to an entropy generation per baryon of $6{\cdot}4 \times 10^6$ k during the cycle.

(5) For a continuum, oscillating, Thomson scattering model which is initially out of equilibrium with $T_{m0} > T_{r0}$, one finds for the final values relative to the initial values a quite new regime (Table IB) as follows:
(a) The numerical value of the rate of change of the scale factor is decreased.
(b) The total energy density is decreased.
(c) The model is closer to equilibrium.
(d) The entropy is increased.

In the models discussed in this work, and in many other cosmological studies, the dominant interaction between the matter and radiation is the Thomson scattering of the photons and free electrons. In Chapter 4 a more general interaction was developed by taking into account the fact that at high radiation temperatures $T_r > 10^7$ K, the scattering cross section of the electron is no longer a constant but becomes dependent on the incident radiation frequency (the Klein-Nishina cross section must then be adopted), and for electron velocities approaching the speed of light $v \sim c$, one must include the relativistic Doppler effect on the incident radiation frequency. This leads to a relativistic, quantum-mechanical expression, the Klein-Nishina interaction, for the electron-photon momentum transfer rate.

A comparison is made between the Klein-Nishina interaction and the classical Thomson interaction by numerically computing for both cases the theoretical momentum transfer rate from the radiation to the electrons for two examples ; (i)a single electron moving at velocity v through blackbody radiation at temperature T_r (Figure 7) and, (ii) an equilibrium distribution of electrons at a temperature T_e interacting with blackbody radiation (Figures 8 and 9). Graphical information is presented in each case and the results can be summarised as follows :

(6) At radiation temperatures $T_r < 10^7$ K and electron velocities $v < 0{\cdot}1\,c$, the classical Thomson expression for the electron's momentum transfer rate is in good agreement with the relativistic, quantum-mechanical Klein-Nishina approach (Figures 7 and 9).

(7) The Klein-Nishina interaction has a weaker radiation temperature dependence than the T_r^4 - law of the classical Thomson case. At radiation temperatures $T_r > 10^7$ K and with v kept constant, the Klein-Nishina formula predicts a less rapidly increasing momentum transfer rate with increasing T_r than that predicted by the Thomson scattering interaction (Figure 7). In particular at $T_r = 10^{12}$ K and $v = 10$ cm s^{-1}, the reduction is of order 5×10^{-3} below the Thomson value.

(8) The Klein-Nishina interaction has a stronger dependence on the electron velocity v than the linear velocity dependence of the classical theory. At electron velocities $v > 0{\cdot}1\,c$ and with T_r kept constant, the Klein-Nishina expression predicts a more rapidly increasing momentum transfer rate with increasing v than that predicted by the Thomson interaction. In particular at $T_r = 10^{12}$ K and with v increased from 10 cm s^{-1} to $0{\cdot}9c$, the Klein-Nishina interaction predicted a ~ 5 times greater increase in the transfer rate than the corresponding increase predicted by the Thomson interaction (Figure 7).

(9) For an equilibrium distribution of electrons at temperature T_e interacting with blackbody radiation at temperature T_r, the momentum exchange between the electrons and radiation increased with increasing T_e and T_r. At constant T_e the Klein-Nishina interaction predicted the drag on the electrons to increase less rapidly with each increase in T_r, whereas for constant T_r the drag increased more rapidly with each increase in T_e (Figure 8).

(10) For a distribution of electrons in thermal equilibrium with radiation, $T_e = T_r \equiv T$, one finds (Figure 9):
(a) At temperatures $T < 10^7$ K the Thomson and Klein-Nishina approaches give similar results for the electron–radiation momentum exchange.
(b) At temperatures $10^7\ \text{K} < T < 5 \times 10^9$ K the Klein-Nishina interaction predicted a lower momentum transfer rate than the corresponding classical Thomson case, i.e., the Klein-Nishina interaction has the electrons and radiation more weakly coupled at these temperatures than the corresponding classical prediction.
(c) At high temperatures $T > 5 \times 10^9$ K, the Klein-Nishina expression predicted the momentum transfer rate to increase rapidly with increasing T and consequently to rise above the value predicted by the Thomson formula, i.e., at high temperatures the Klein-Nishina interaction predicts the electrons and radiation to be more strongly coupled than the corresponding classical Thomson interaction prediction.

(11) Many cosmological studies begin at temperatures much greater than 10^7 K, so the Klein-Nishina interaction ought to be used in these circumstances. In the cosmological models discussed here the Klein-Nishina interaction, like the Thomson interaction, is easily capable of maintaining thermal equilibrium between the matter and radiation.

We end this report by considering which parts of the work are open to further discussion and investigation.

A nonstandard feature of the continuum-particle model was the prediction of a neutrino temperature slightly above the radiation temperature. In particular, at the present epoch with $T_r = 2{\cdot}70$ K then $T_\nu = T_r/0{\cdot}9857$, whereas the standard model has $T_\nu = T_r/1{\cdot}404$ at this epoch (Peebles 1966; Wagoner, Fowler, and Hoyle 1967).

A higher neutrino temperature would have important consequences for the universal mass density and for the mass density on scales of clusters of galaxies. Ordinary nucleonic matter appears incapable of accounting for the dynamically inferred mass on the scales of galactic clusters, and this mass discrepancy may persist down to scales of binary galaxies (Faber and Gallanger 1979). It has been suggested that relic neutrinos, clustering on large scales, could account for the hidden mass. Calculations show that if the neutrinos have a temperature $T_\nu = T_r/1{\cdot}404$ at the present epoch then the mass discrepancy can be accounted for by neutrinos if the neutrino mass falls within the limits $4\ \text{eV} < m_\nu < 20\ \text{eV}$, and if they have small mass $m_\nu < 1{\cdot}4\ \text{eV}$ then the neutrinos could still dominate the universal mass density (Schramm and Steigman 1981).

The number density of relic neutrinos depends sensitively on the temperature during the early universe because $n_\nu \propto T_\nu^3$. Hence a higher T_ν would significantly

increase the number of primordial neutrinos and would lower the limits imposed on m_ν for the neutrinos to dominate the universal mass density. Also, more neutrinos would participate in gravitational collapse, giving lower constraints on m_ν for the neutrinos to make up the mass discrepancy in galactic clusters.

Both closed, $K = 1$, and open, $K = -1$, model universes have been studied in this work. The closed models could be investigated further by taking them through additional cycles. This would not be possible however, for the continuum-particle model because the final temperature on contraction, $2{\cdot}1 \times 10^9$ K, was inadequate to decompose the H_e^4. To take the final state as the starting point for a second cycle would not be reasonable since further contraction would have meant higher temperatures and with the H_e^4 nuclei eventually breaking up. To investigate further cycles would require additional work on the decomposition of the elements on contraction.

In all the interacting oscillating models discussed here which began in thermal equilibrium, the entropy S increased during both the expanding and contracting phases, and the model collapsed to the initial scale factor with a greater total energy U and a greater $|\dot{R}|$ value than with which it started. However the dependence of the energy and entropy generated during a cycle on the model's initial data requires further study. Also, if the oscillating model is taken through many expansions and contractions, would the entropy and total energy increase with each cycle and without limit? If the total energy U is increased with each cycle then the scale factor at the point of maximum expansion R_{max} would increase with each cycle because, by equation (2.2), one has $R_{max} \propto U$ at the instant $\dot{R} = 0$ (note that this multicycle argument assumes that the end of one, truncated, cycle can be connected to the beginning of the next cycle by taking the data at the final contraction point as the initial conditions for the next cycle; the region close to the singularity having been 'cut out' by the model).

An extrapolation back to earlier cycles would imply that each successive earlier cycle contains less energy and entropy and expands to a smaller scale factor R_{max} than its neighbouring later cycle. How far back could this be taken ? It suggests that a very early cycle would be essentially devoid of energy and entropy and undergo only a small oscillation. The creation of energy and entropy would occur through repeated oscillations, with the maximum scale factor increasing with each later cycle. This multicycle model possesses therefore an infinite future but only a finite past.

INDEX OF SYMBOLS

AND

REFERENCES

INDEX OF SYMBOLS

Physical constants

Velocity of light	$c = 2{\cdot}9979 \times 10^{10}$ cm s^{-1}
Gravitational constant	$G = 6{\cdot}6732 \times 10^{-8}$ dyn cm^2 g^{-2}
Boltzmann constant	$k = 1{\cdot}3806 \times 10^{-16}$ erg $^oK^{-1}$
Planck	$h = 6{\cdot}6262 \times 10^{-27}$ erg s
Electronic charge	$e = 4{\cdot}8033 \times 10^{-10}$ esu
Electron mass	$m_e = 9{\cdot}1096 \times 10^{-28}$ g
Proton mass	$m_p = 1{\cdot}6725 \times 10^{-24}$ g
Neutron mass	$m_n = 1{\cdot}6749 \times 10^{-24}$ g
Blackbody constant	$a = \frac{8}{15}\frac{\pi^5 k^4}{c^3 h^3}$ $= 7{\cdot}5641 \times 10^{-15}$ erg cm^{-3} $^oK^{-4}$
Thomson cross section	$\sigma_{Th} = \frac{8}{3}\pi\left(\frac{e^2}{m_e c^2}\right)^2$ $= 6{\cdot}6525 \times 10^{-25}$ cm^2
Curvature index	$K = +1, 0, -1$

Variables

t	-	time
R	-	scale factor
U_i	-	total energy of component i
ρ_i	-	mass density of component i
T_i	-	temperature of component i
p_i	-	pressure of component i

S_i - entropy of component i

ε_i - rate of energy transfer to component i

N_i - total number of particles type i

m_i - mass of particle type i

E_i - total energy of a particle type i

g_i - number of spin states of particle type i

$X_i = \frac{N_i}{N_b}$ abundance by number of particles type i to the total number of baryons

$M_i = \frac{N_i m_i}{N_b m_b}$ abundance by mass of particles type i to the total mass of baryons

T_f^i - the 'freezing-in' temperature of element type i

All extensive variables used in the continuum and continuum-particle models refer to a comoving volume $V(t)$,

$$V(t) = \iiint_{r\,\theta\,\phi} \sqrt{-g}\; dr\, d\theta\, d\phi \,,$$

where g is the determinant of the spacelike part of the Robertson-Walker metric (Robertson 1936; Walker 1936),

$$ds^2 = c^2 dt^2 - R^2(t) \left[\frac{dr^2 + r^2(d\theta^2 + \sin^2\theta\, d\phi)}{\left(1 + \frac{Kr^2}{4}\right)^2} \right] ,$$

and where r, θ, and ϕ are the comoving coordinates. $R(t)$ is the scale factor at time t, and the limits of integration on the volume $V(t)$ are so chosen that

$$V(t) = \frac{4}{3}\pi R^3(t) \,.$$

REFERENCES

Aaronson, M., Mould, J., Huchra, J., Sullivan, W.T., Schommer, R.A. and Bothun, G.D. 1980, Ap. J., 239, 12.

Abramowitz, M. and Stegun, A. 1972, Handbook of Mathematical Functions (New York: Dover).

Alpher, R.A., Bethe, H.A. and Gamow, G. 1948, Phys. Rev., 73, 803.

Alpher, R.A. and Herman, R.C. 1950, Rev. Mod. Phys., 22, 153.

Anderson, J.L. and Witting, H.R. 1973, Trans. New York Acad. Science, 35, 636.

Bahcall, N.A. and Soneira, R.M. 1982, Ap. J., 262, 419.

Baierlein, R. 1971, Atoms and Information Theory (San Francisco: Freeman), Chapters 4 and 8.

Balzano, V.A. and Weedman, D.W. 1982, Ap. J., 255, L1.

Bludman, S.A. 1976, Gen. Rel. Grav., 7, 569.

Bond, J.R., Szalay, A.S., and Turner, M.S. 1982, Phys. Rev. Letts., 48, 1636.

Bondarenko, L.N., Kurguzov, V.V., Prokof'ev, Yu.A., Rogov, E.V., and Spivak, P.E. 1978, Soviet Phys.-JETP Letts., 28, 303.

Cabibbo, N., Farrar, G.R., and Maniani, L. 1981, Phys. Letts., 105B, 155.

Chandrasekhar, S. 1939, An Introduction to the Study of Stellar Structure (Chicago: University Press), Chp. 10.

Cohen, J.M. 1967, Nature, 216, 249.

Cowsik, R. and McClelland, J. 1972, Phys. Rev. Letts., 27, 669.

Davidson, W. 1962, Mon. Not. Roy. Astr. Soc., 124, 79.

Davis, M., Huchra, J., Latham, D.W., and Tonry, J. 1982, Ap. J., 253, 423.

Davis, M., Tonry, J., Huchra, J., and Latham, D.W. 1980, Ap. J., 238, L113.

Dolgov, A. and Zeldovich, Ya. B. 1981, Rev. Mod. Phys., 53, 1.

Dicus, D.A., Letaw, J.R., Teplitz, D.C., and Teplitz, V.L. 1982, Ap. J., 252, 1.

Donald, J.A. 1978, Annals of Phys., 110, 251.

Dooren, Van P. and Ridder, De L. 1976, J. Comp. Appl. Math., 2, 207.

Einstein, A. 1916, Ann. der Physik, 49, 769.

Emslie, A.G. and Green, R.M. 1978, Ap. Sp. Sci., 58. 181.

Faber, S.M. and Gallanger, J.S. 1979, Ann. Rev. Astr, Ap., 17, 135.

Fanti, C., Lari, C., and Olori, M.C. 1978, Astr. Ap., 61, 487.

Felton, J.E. and Morrison, P. 1966, Ap. J., 146, 686.

Field, G.B. 1976, Frontiers of Astrophysics, ed. E.H. Avrett, (Cambridge, U.S.A.: Harvard University Press).

Ford, H.C., Harms, R.J., Ciardullo, R., and Bantko, F. 1981, Ap. J., 245, L53.

Friedmann, A. 1922, Z. Physik, 10, 377.

Gautier, D. and Owen, T. 1983, Nature, 302, 215.

Gott, J.R., Gunn, J.E., Schramm, D.N., and Tinsley, B.M. 1974, Ap. J. 194, 543.

Heitler, W. 1954, The Quantum Theory of Radiation (Oxford: Oxford University Press), Section 22.

Hönl, H. 1971, In Perspectives in Quantum Theory, ed. W. Yourgrau and A. Van Der Merwe (Cambridge, U.S.A.: MIT Press), Chapter 8.

Hubble, E.P. 1925, Ap. J., 62, 409.

_____. 1929, Proc. Nat. Acad. Sci. U.S.A., 15, 168.

_____. 1936, Ap. J., 84, 517.

Hubble, E.P., and Humason, M.L. 1931, Ap. J., 74, 43.

Humason, M.L., Mayall,N.Q., and Sandage, A.R. 1956, Astron. J., 61, 97.

Ipser, J. and Sikivie, P. 1983, Phys. Rev. Letts., 50, 925.

Jackson, J.D. 1962, Classical Electrodynamics (New York: Wiley), Section 11·4 .

Kinman, T.D. and Davidson, K. 1982, Phil. Trans. Roy. Soc. A, 307, 37.

Kirshner, R.P., Oemler, A., Schechter, P., and Shectman, S.A. 1981, Ap. J., 248, L57.

Kristian, J., Sandage, A., and Westphal, J.A. 1978, Ap. J., 221, 383.

Landsberg, P.T. 1965, In Problems in Thermodynamics and Statistical Physics, ed P.T. Landsberg (London: Pion Ltd.), Chapters 3 and 5.

Landsberg, P.T. and Park, D. 1975, Proc. Roy. Soc. A, 346, 485.

Landsberg, P.T. 1978, Thermodynamics and Statistical Mechanics (Oxford: Oxford University Press), Chapter 9.

Landsberg, P.T. and Reeves, G.A. 1980, in Proc. 9th Int. Conference on General Relativity and Gravitation, Jena, GDR.

Landsberg, P.T. and Reeves, G.A. 1982, Ap. J., 262, 432.

Lee, B.W. and Weinberg, S. 1977, Phys. Rev. Letts., 39, 165.

Lemaître, G. 1927, Ann. Soc. Sci. Bruxelles, 47A, 49.

_____. 1931, Mon. Not. Roy. Astr. Soc., 91, 490.

Linscott, I.R. and Erkes, J.W. 1980, Ap. J., 236, L109.

Lyubimov, V.A., Novikov, E.G., Nozik, V.Z., Tretyakov, E.F., Kozik, V.S., and Myasoedov, N.F. 1981, Soviet Physics-JETP, 54, 616.

May, T.L. and McVittie, G.C. 1970, Mon. Not, Roy. Astr. Soc., 148, 407.

_____. 1971, Mon. Not. Roy. Astr. Soc., 153, 491.

McIntosh, C.B.G. 1968, Mon. Not. Roy. Astr. Soc., 138, 423.

Melott, A.L. 1983, Ap. J., 264, 59.

Milne, E.A. 1935, Relativity, Gravitation, and World Structure (Oxford: Oxford University Press), p73.

Misner, C.W., Thorne, K.S., and Wheeler, J.A. 1973, Gravitation (San Francisco: Freeman), Chapter 27.

Neugebauer, G. and Meier, W. 1976, Ann. der Physik, 33, 161.

Olive, K.A., Schramm, D.N., Steigman, G., Turner, M.S., and Yang, J. 1981, Ap. J., 246, 557.

Pagel, B.E.J. 1982, Phil. Trans. Roy. Soc. A, 307, 19.

Park, D. 1973, Collective Phen., 1, 71 and 111.

Partridge, R.B. 1980, Ap. J., 235, 681.

Patterson, T.N.L. 1968, Math. Computation, 22, 847 and 877.

Pauli, W. 1958, Theory of Relativity, (Elmsford, New York : Pergamon), Section 49.

Peach, J.V. 1970, Ap. J., 159, 753.

Peebles, P.J.E. 1966, Ap. J., 146, 542.

_____. 1968, Ap. J., 153, 1.

_____. 1971, Physical Cosmology (Princeton: Princeton University Press), Chapter VII.

_____. 1980, The Large-Scale Structure of the Universe (Princeton: Princeton University Press), Chapter I.

Penzias, A.A. and Wilson, R.W. 1965, Ap. J., 142, 419.

Petrosian, V. 1982, Nature, 298, 805.

Pinkau, K. 1980, Astr. Ap., 87, 192.

Pomraning, G.C. 1973, Radiation Hydrodynamics (Elmsford, New York: Pergamon), Chapter VII.

Press, W.H. and Davis, M. 1982, Ap. J., 259, 449.

Reeves, G.A. and Landsberg, P.T. 1982, Ap. J., 259. 25.

Rephaeli, Y. 1982, Phys. Rev. D, 26, 770.

Robertson, H.P. 1936, Ap. J., 83, 187 and 257.

Rood, R.T., Wilson, T.L., and Steigman, G. 1979, Ap. J., 227, L101.

Sandage, A.R. 1968, Ap. J., 152, L149.

Sandage, A.R. and Tammann,G.A. 1982, Ap. J., 256, 339.

Sandage, A.R., Tammann,G.A., and Hardy, E. 1972, Ap. J., 172, 253.

Sanduleak, N. and Pesch, P. 1982, Ap. J., 258, L11.

Scheid, F. 1968, Numerical Analysis (New York: McGraw Hill, Schaum), Chapter 20.

Schmidt, H. 1966, J. Math. Phys., 7, 494.

Schramm, D.N. and Steigman, G. 1981, Ap. J., 243, 1.

Schumacher, D.L. 1964, Proc. Camb. Phil. Soc., 60, 575.

Sciama, D.W. 1982, Phys. Letts., 114B, 19.

Searle, L. and Sargent, W.L.W. 1972, Comments Ap. Sp. Phys., 4, 59.

Seldner, M. and Peebles, P.J.E. 1978, Ap. J., 225, 7.

Slipher, V.M. 1914, Lowell (Flagstaff) Obs. Bull., 58.

Spite, M. and Spite, F. 1982, Nature, 297, 483.

Stecker, F.W. and Shafi, Q. 1983, Phys. Rev. Letts., 50, 928.

Steigman, G. 1982, Phil. Trans. Roy. Soc. A, 304, 97.

Symbalisty, E.M.D., Yang, J., and Schramm, D.N. 1980, Nature, 288, 143.

Szekeres, P. and Barnes, A.S. 1979, Mon. Not. Roy. Astr. Soc., 189, 767.

Taylor, R.J. 1980, Rep. Prog. Phys., 43, 253.

Tolman, R.C. 1931, Phys. Rev., 38, 797.

_____. 1934, Relativity, Thermodynamics and Cosmology (Oxford: Oxford University Press), Sections 130, 131, and 166-175.

Tubbs, A.D. and Wolfe, A.M. 1980, Ap. J., 236, L105.

Tucker, W.H. 1975, Radiation Processes in Astrophysics (Cambridge, U.S.A.: MIT Press), Chapter 4.

Tyson, J.A. and Jarvis, J.F. 1979, Ap. J., 230, L153

Uson, J.M. and Wilkinson, D.T. 1982, Phys. Rev. Letts., 49, 1463.

Vaucouleurs, G. 1982, Nature, 299, 303.

Vidal-Majdar, A., Laurent, C., Bonnet, R.M., and York, D.G. 1977, Ap. J., 211, 91.

Wagoner, R.V. 1973, Ap. J., 179, 343.

Wagoner. R., Fowler, W., and Hoyle, F. 1967, Ap. J., 148, 3.

Walker, A.G. 1936, Proc. London Math. Soc., 42, 90.

Weinberg, S. 1972, Gravitation and Cosmology (New York: Wiley), Chapter 15.

_____. 1974, Rev. Mod. Phys., 46, 255.

_____. 1982, Phys. Rev. Letts., 48, 1303.

Weyl, H. 1923, Phys. Z., 24, 230.

Weymann, R. 1965, Phys. Fluids, 8, 2112.

Wienke, B.R. 1975, Am. J. Phys., 43, 317.

Yahil, A., Sandage, A., and Tammann, G.A. 1980, Phys. Scripta, 21, 635.

Zeldovich, Ya. B., Einasto, J., and Shandarin, S.F. 1982, Nature, 300, 407.

The following published papers were included in the bound thesis. These have not been digitised due to copyright restrictions, but the links are provided.

Reeves, G.A. Landsberg, P.T. (1982) **Thermal interaction between matter and radiation in the early universe** The Astrophysical Journal: 259, 25-29

https://doi.org/10.1086/160142

Reeves, G.A. Landsberg, P.T. (1982) **Heat death and oscillation in model universes containing interacting matter and radiation** The Astrophysical Journal: 262, 432-441

https://doi.org/10.1086/160438